550

THE STUDY OF FLOODING CORRELATIONS OF COUNTER-CURRENT TWO-PHASE FLOW IN A VERTICAL TUBE UNDER ELECTRIC FIELD

THE STUDY OF FLOODING CORRELATIONS OF COUNTER-CURRENT TWO-PHASE FLOW IN A VERTICAL TUBE UNDER ELECTRIC FIELD

by

S.T.REVANKAR

Part A : McMaster Project *

A Report Submitted to the School of Graduate Studies in Partial Fulfilment of the Requirements for the Degree of Master of Engineering

McMaster University

1982

*One of the two project reports -- the other part is designated as Part B : Industrial Project (off compus)

MASTER OF ENGINEERING (1982) MCMASTER UNIVERSITY

Hamilton, Ontario

TITLE : The Study of Flooding Correlations of Counter-Current Two-Phase Flow in a Vertical Tube Under Electric Field

AUTHOR : S.T.Revankar,M.Sc.(Karnatak)

SUPERVISOR : Dr. J.S.Chang

NUMBER OF PAGES : ix , 73.

ABSTRACT

A counter-current two-phase flow under an applied electric field has been studied theoretically using potential flow equations. A flooding correlation has been derived taking account of applied electric field on the interface for both adiabatic and condensing system. It is found that the electric field enhances flooding phenomena in case of adiabatic system. In the case with system involving condensation the electric field enhances flooding at low liquid flow rates and at high liquid flow rates the flooding point decreases under electric field depending on the rate of subcooling.

ACKNOWLEDGEMENT

The author would like to express his deep sense of gratitude to Dr.J.S.Chang for his inspiring discussions, suggestions and guidence while carrying the present work. Thanks are also due to Mr.R.Girard for his help.

TABLE OF CONTENTS

NOMENCLATURE

Symbol	Description
C	Constant in klallis and Dutateladze correlation.
c	wave speed
C_p	specific heat
D	tube inner diameter
D_H	hydraulic diameter
D_o	electric displacement
D*	Bond number
E	electric field intensity
e_x, e_y, e_z	components of electric field in x, y, z directions
f_i	interfacial friction factor
f_w	wall friction factor
g	acceleration due to gravity
h_E	heat transfer coefficient with electric field
h_o	heat transfer coefficient without electric field
h_{fg}	latent heat of condensation
i_x, i_y, i_z	unit vectors in x, y, z directions
j_g	superfacial gas flux
j_f, j_l	superfacial liquid velocity
k_x, k_y, k_z	wave vectors in x, y, z directions
K_l	liquid Kutateladze number
K_g	gas Kutateladze number
k	wave number
k_c	critical wave number
m	parameter in Wallis correlation

NOMENCLATURE (Continued)

$\bar{n}$	unit normal vector
p, P	pressure
R	entry radius
Re_f	liquid Reynolds number
Re_g	gas Reynolds number
Re_Γ	liquid film Reynolds number
T	temperature
U	mean velocity
V	velocity of either phase (gas or liquid)
V_x, V_y, V_z	velocity components
(x,z)	plane normal to the tube
y	distance along the tube
$z(\phi)$	parameter for enhancement of condensation under electric field
ξ	surface variation of interface
η	amplitude of purterbation
θ	angle of tube end cutting
β	dielectric constant
α, ϵ_g	void fraction
δ	mean liquid thickness
μ	dynamic viscosity
σ	surface tension
ρ	density
ω	frequency
λ_c	critical wavelength

NOMENCLATURE (Continued)

ϕ	non-dimensional electric field
τ	shear stress

Subscripts

g	gas
f,l	liquid
sat	saturation
sub	subcooling
cond	condensation
w	wall
(0), (1), (2)..	perterbation of order 0, 1, 2, ...

Superscripts

*	non-dimensional quantity
c,d,e,f	values of variable at point c,d,e,f

Abbreviations

LWR	Light Water Reactor
LOCA	Loss of Coolant Accident
ECC	Emergency Core Cooling
BWR	Boiling Water Reactor
CCFL	Counter Current Flooding Limit

CHAPTER 1

INTRODUCTION

In many industrial process components, such as wetted columns, liquid film evaporators and updraft condensers, counter-current gas-liquid two-phase flow have been observed and actively used. In such systems, the liquid flow is limited depending on gas flow rates, which is generally referred as 'counter-current flow limit' (CCFL) or 'flooding'. This phenomenon is usually accompanied by a chaotic flow pattern within the channel and may involve sudden change in the system pressure, leading to departure from steady operation of the system.

Recently flooding has become one of the major subjects of study in relation to the loss of coolant accident in nuclear power plant primary heat transport loops. However, little attention has been paid in monitoring flooding phenomena by external influences. The present work is an effort to study the effects of external electric field on counter-current gas-liquid annular flow in regime of flooding. Such systems exist in nuclear fusion reactor [66], new type of emergency nuclear reactor core cooling system [67] and various industrial processes [68].

1.1 Definition of Flooding

In modeling the flooding phenomena, the criterion for setting the flooding point depends upon the definition of flooding. Here, we try to analyze the flooding mechanism and define flooding accordingly. In flooding phenomenon, two concepts play important roles: first, the interfacial instability and entrainment, and second, the flow limitation

of either phase. In Fig. 1.1, the relationship between the liquid and the gas flow rates in a general two-phase counter-current flow system is shown. Region 1 represents the flow regime where the stable operation of the system can be observed. In region 2, the continous operation of the two-phase counter-current flow system is not possible. Thus, for a given liquid flow rate, there exists a limit to which the gas flow can penetrate through the channel and vice-versa. The locus of these flooding points forms an envelope of all maximum flow rates of the two-phase flow system and this curve is called 'flooding curve'.

To characterize the flow regimes associated with flooding phenomena, the relative magnitudes of interfacial and wall shear stresses have been considered in annular counter-current gas-liquid flow [8], as shown in Fig. 1.2. For small gas-flow rates, a smooth falling liquid film is observed. On increasing the gas flow rate, small disturbance waves appear on the film. These are particularly significant at the gas inlet. A further increase in gas velocity causes the waves at the gas inlet to bridge across the tube and an intermittent churn flow is established; however, some liquid still flows down. A further gas velocity increase will lead to complete hold-up of liquid accompanied by a dramatic change in pressure drop across the tube, this point is commonly taken as total flooding point. Thus, it can be seen that the start of flow limitation occurs right from the region where the disturbance waves appear on the liquid film, and this region is the one at which the interface shear stress is more than the wall shear stress as shown in Fig. 1.2.

Now, the flooding phenomena may be defined in the following way with characterization criteria:

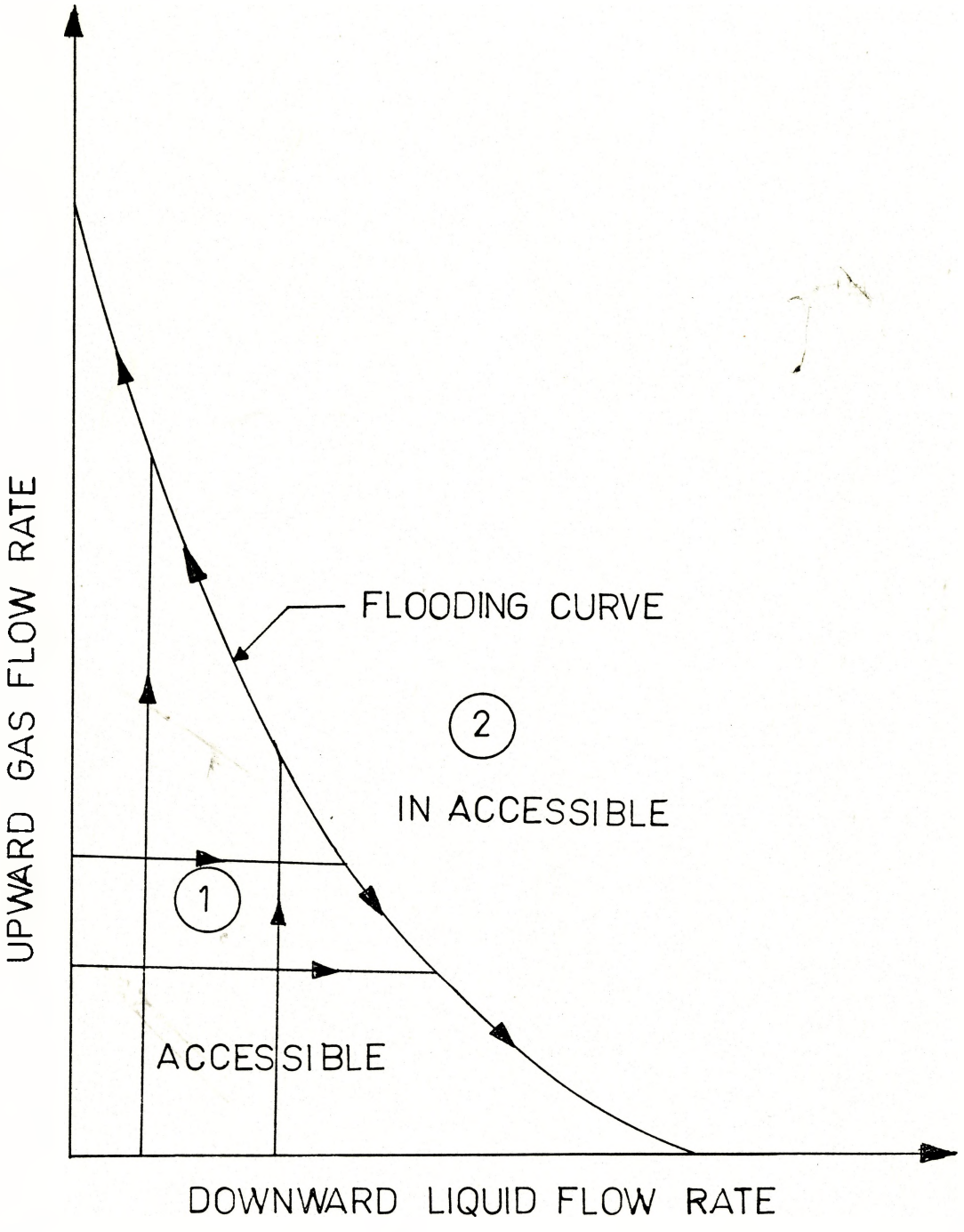

Figure 1.1 Flooding in vertical two-phase counter-current flow system.

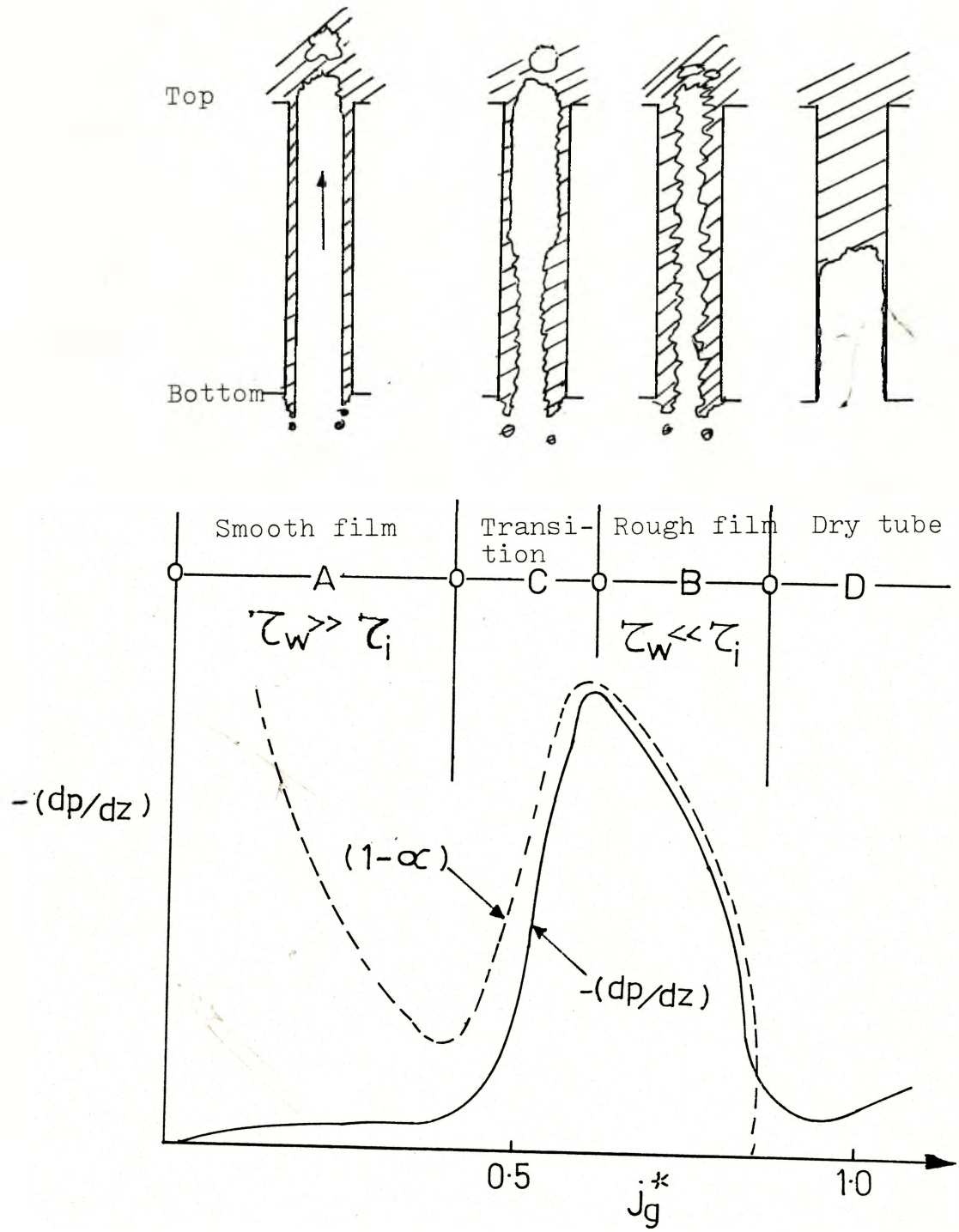

Figure 1.2 Typical variation of pressure gradient and liquid fraction with gas flux. The corresponding film thickness distribution in the tube are shown above.

a) Transition to flooding: A region where the interfacial shear stress τ_i is comparable with the wall shear stress τ_w impeding on the liquid flow. Therefore, the disturbance waves appear on the liquid surface [69] (Fig. 3.a).

b) Intermediate flooding: A region where $\tau_i >> \tau_w$ and the interface is agitated and the liquid phase near interface is transported in an upward directon by a strong upward gas flow (Fig. 3.b).

c) Partial flooding: A region where the curves on liquid film, grow to form a liquid bridge across the channel, and then some portion of the liquid is transported in upward direction by gas flow to form intermittent churn (Fig. 3c).

d) Total flooding: A region where the downward flow of liquid is totally stopped and the large pressure drop across the tube is expected (Fig. 3.d).

In the case of non-adiabatic system, where the gas is steam/vapour, the effect of vapour condensation on the counter-current flow limiting phenomena have to be considered. In such systems, it is expected that the presence of a large amount of condensation stress on the liquid film surface. As well, the entrainment of liquid droplets associated with intermediate and partial flooding may be enhanced due to condensation and would lead to complicated flow patterns. Especially in reflux condensation, these features are associated with periodic flow instabilities [9].

1.2 Two-Phase Flow Under Electric Field

Most of the studies so far carried in two-phase flow involving electric field are in the interest of enhancement of heat transfer, e.g.

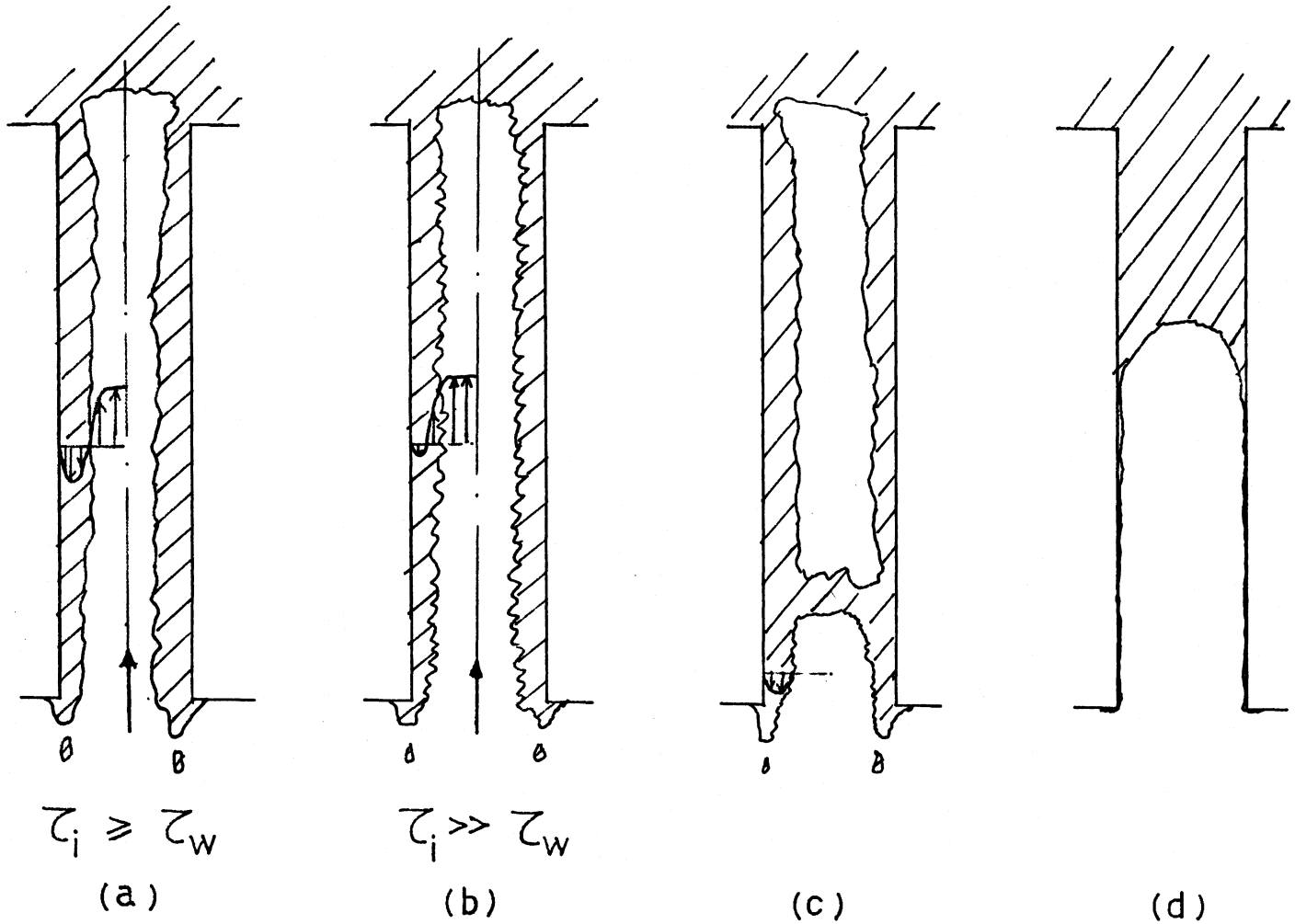

Figure 1.3 Flooding regimes defined with flow patterns depending on shear stresses.

boiling, condensation, etc. In the boiling heat transfer the applied electric field has been found to affect the dynamic behaviour of the interface separating vapour and liquid phases of the boiling fluid [1,2]. Thus, a control on the phenomenon of hydrodynamic stability by an applied electric field is established and an increase in heat transfer could be achieved.

Similarly, in condensation phenomena, the enhancement of heat transfer even to the order of ten-fold has been observed with applied electric field [3,4,5]. The mechanism of condensation enhancement with electric field may be due to the decreasing of film thickness, enhancement of homogeneous condensation, increasing the condensation surface due to the appearance of the conically shaped droplets, enhancement of electrohydrodynamic flow, and increase of the turbulence in the film by enhancement of interfacial instability.

The principal consequence of interest in two-phase heat transfer processes, such as boiling and condensation is the Rayleigh-Taylor type instability. With an external applied electric field, the coupling between the Rayleigh-Taylor type instability and electrohydrodynamical instability leading to total system instability has been observed for stationary gas and liquid system [6]. Another aspect of hydrodynamic instability mechanism called Kelvin-Helmholtz type instability is of considerable importance in two-phase separated flow systems involving high relative velocities. A study of two-phase air-water horizontal flow in tubes under applied electric field has shown that Kelvin-Helmholtz instability mechanism can be coupled electrohydrodynamically to explain the flow patterns such as wavy, slug in horizontal systems [7] (Fig. 1.4).

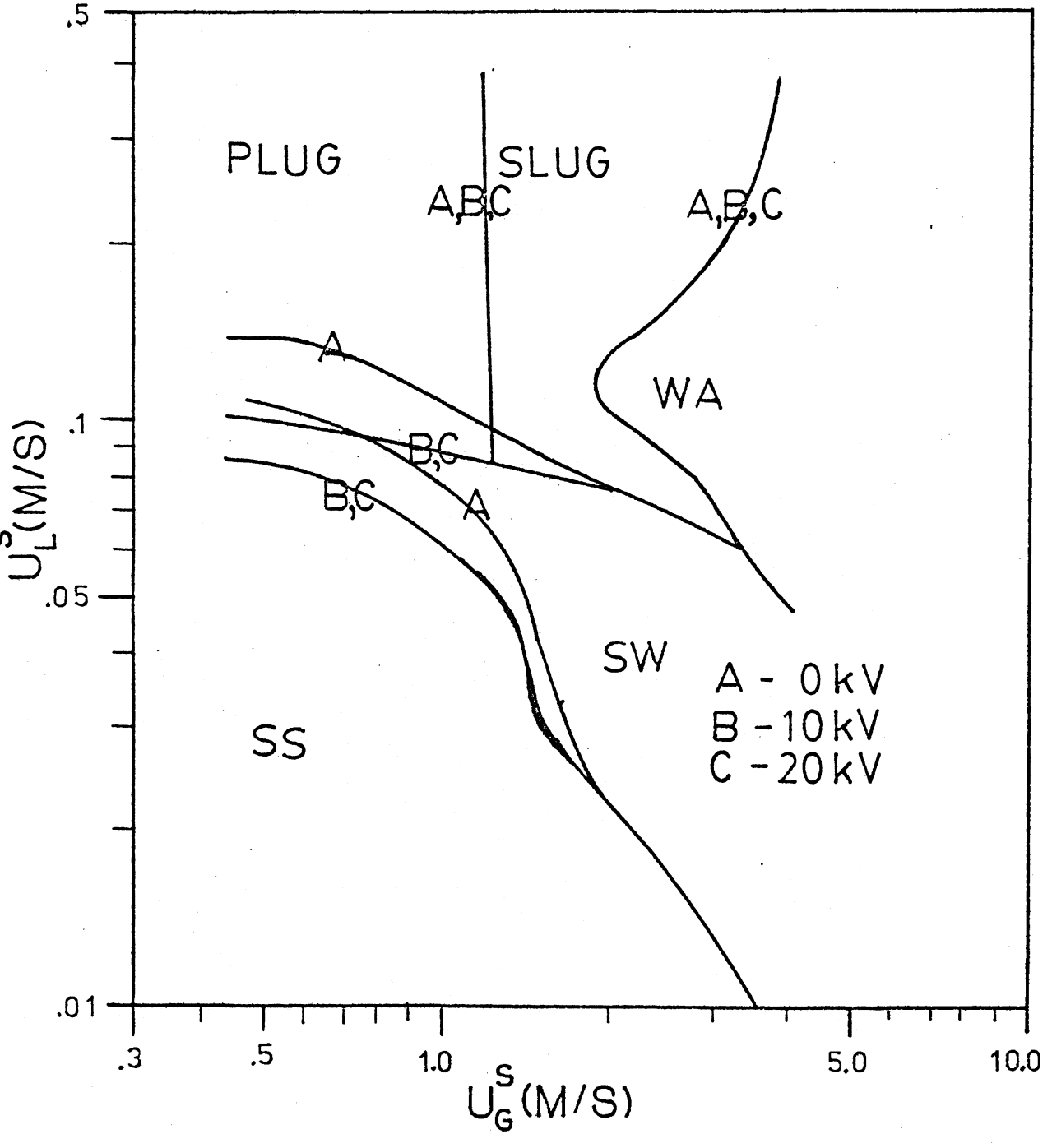

Figure 1.4 Comparison of flow regimes observed in a 0.1127m. internal diameter pipe at different voltages(ref.7).

1.3 Aim and Scope of the Present Work

The present investigation is basically theoretical approach to investigate the flooding phenomena under the presence of externally applied electric field and ultimately arrive at a total flooding correlation to be applicable for counter-current gas and liquid annular flow limitation. For the situation like LOCA, where in the injected emergency core cooling (ECC), water may be blocked by the steam generated in the reactor core through the counter-current flooding condition. By application of external forces such as electric field on suitable locations, the breakdown of the flooding can be achieved through the enhancement of condensation and interface instability in such situations. In Chapter 2, the flooding correlations so far available have been reviewed for counter-current two-phase annular flow, including the effects of entrainment, condensation, etc. In Chapter 3, the analytical modelling of the flooding under the electric field is presented. A flooding correlation obtained is compared with earlier correlations. The condensation effects on flooding are incorporated in Chapter 4. The pertinent discussions and conclusions are given in Chapters 5 and 6, respectively.

CHAPTER 2

FLOODING CORRELATIONS

As a practical approach in engineering discipline, experiments are the most important sources of understanding physical phenomena. The flooding correlations are thus almost based on experimental investigations. As a feedback, analytical modelling for studying have also been carried, which again rely on the experimental data for obtaining practically applicable flooding correlations. Recently extensive review on the counter-current two-phase flooding, have been given by Tien and Liu [47] and Deakin [48] for both the condensing (e.g., steam-water system) and as well for adiabatic systems (e.g. air-water).

For the determination of the flooding point experimentally, some investigators adopted the criterion of zero liquid penetration [18], others took the beginning of the liquid flow reversal [31] and some others took inception of liquid entrainment as their experimental criterion, for the onset of flooding [22], while others took large pressure drop [23]. Because of the varied physical models and adopting different criterion for the onset of flooding in the experiments, there has been considerable discrepancy over existing analytical and experimental studies. In the subsequent sections, the experimental studies and analytical approaches made in arriving at flooding correlations along with various factor affecting the flooding phenomena has been reviewed. In Figure 2.1, the various geometries of the tube ends considered by various authors for experimental work are shown.

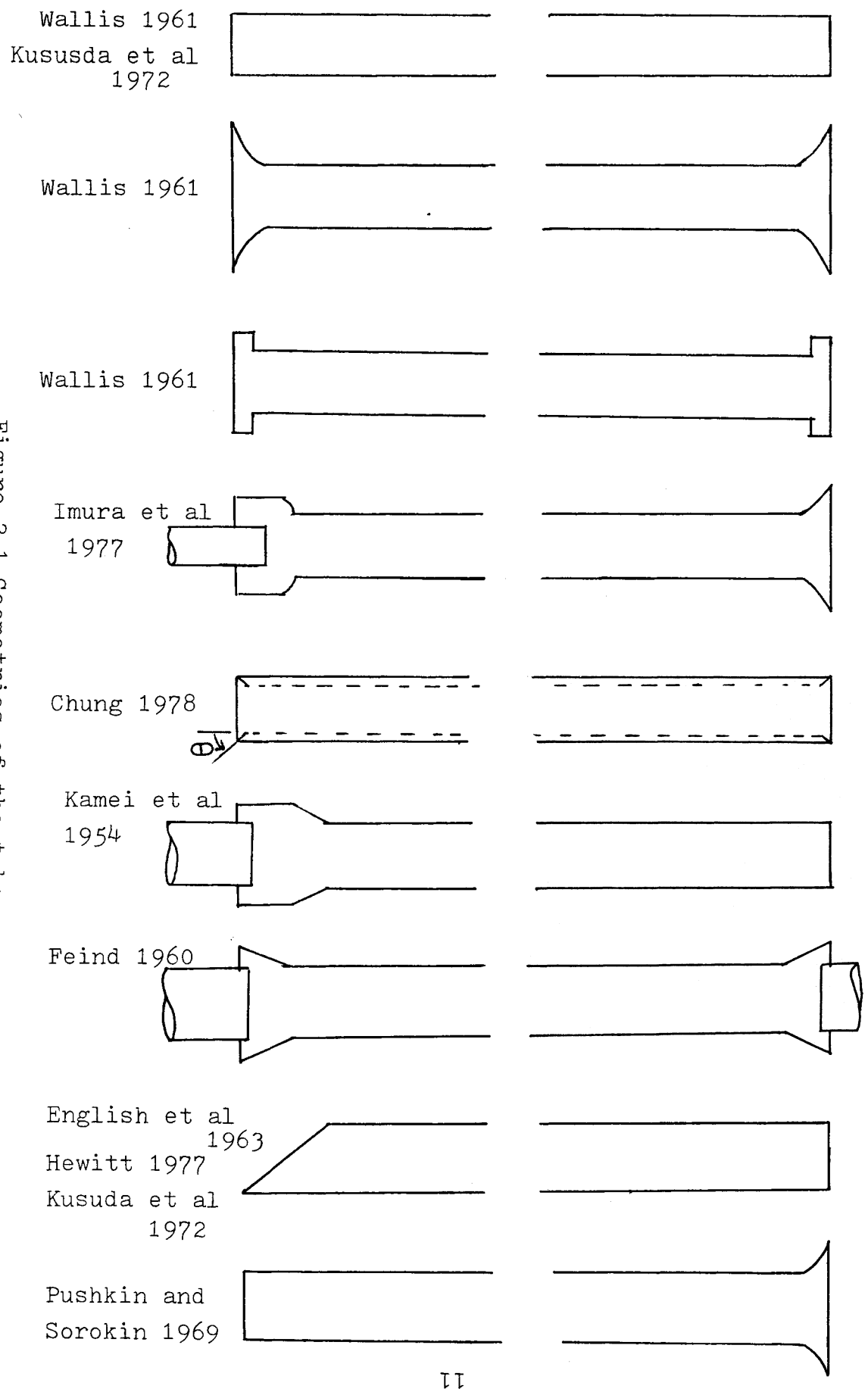

Figure 2.1 Geometries of the tubes.

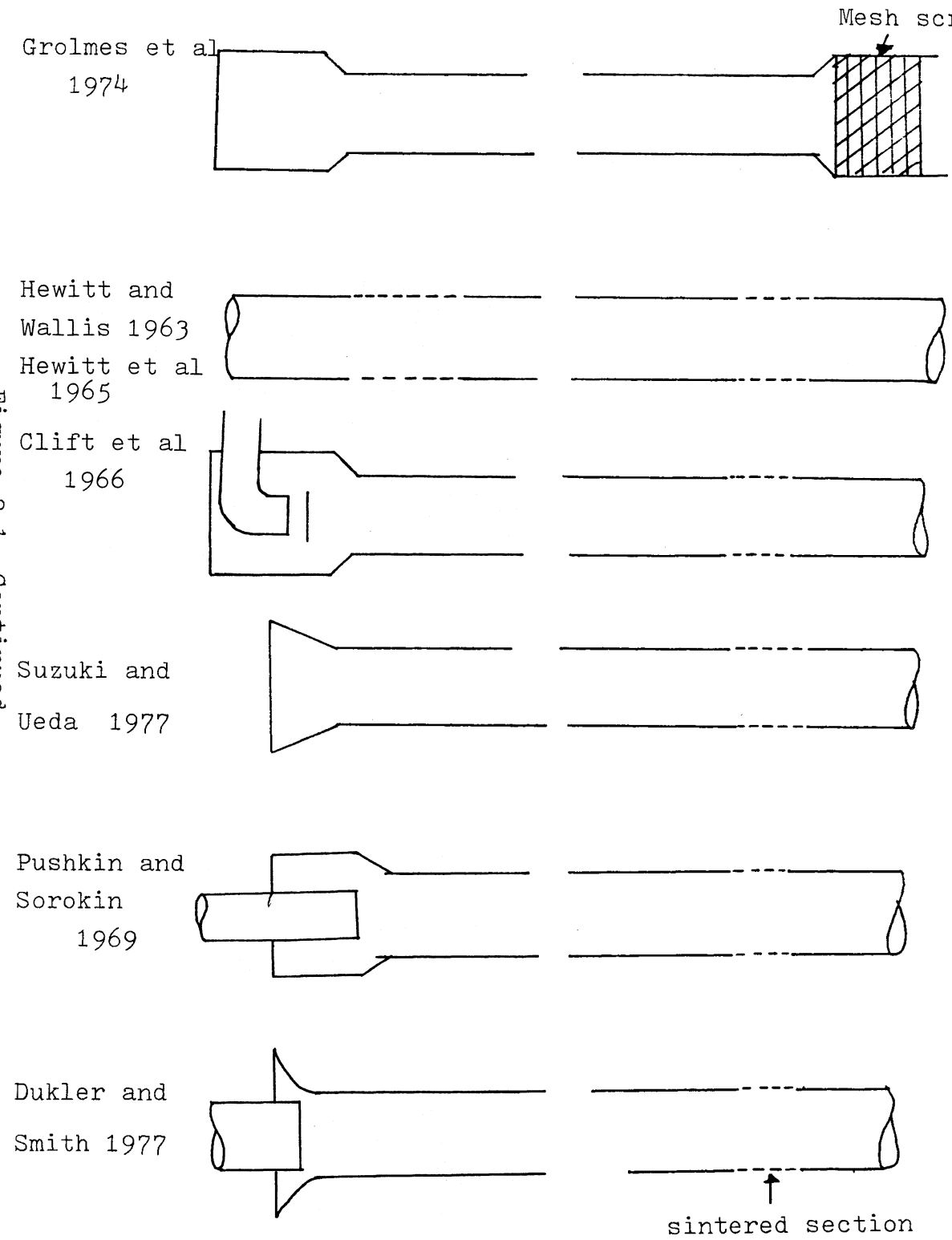

Figure 2.1 Continued.

2.1 Experimental Studies

Much of the earlier works on flooding were encountered in experiments on packed towers [10, 11]. Empirical flooding correlations for gas-liquid counter current flow based on experimental data were given by Kamei et al. [12] for air-water, air-Millet jelly solution, and air-soap solution with a range of liquid Reynolds number from 50 to 700, and by Feind [13] for air-water, air-diethylene glycol solution systems over a liquid Reynolds number range of 0.5 to 3000 (see Table 2.1 for flooding expression). Wallis [14] correlated the experimental data into a empirical equation with a consideration to balance of inertial and hydrostatic forces, which in modified form is

$$j_g^{*1/2} + m j_f^{*1/2} = C \qquad (2.1)$$

where m and C are constants having value between 0.8 to 1 and 0.7 to 1 respectively from experimental observations. Here $j_g^* = j_g \rho_g^{1/2} [Dg(\rho_f-\rho_g)]^{-1/2}$, $j_f^* = j_f \rho_f^{1/2} [Dg(\rho_f-\rho_g)]^{-1/2}$ are dimensionless velocities of gas and liquid respectively and D is diameter of the tube. For air-water system the test results showed that the tube diameter and entrance conditions, reflected in the constant c, are important in flooding. The liquid flooding velocity was found [15] to reduce with decreasing viscosity of fluids. The experimental data by Clift et al. [16], showed agreement with Wallis correlation with C = 0.79 and m = 0.84 or $(j_g^*)^{1/2} + 0.84\ (j_f^*)^{1/2} = 0.79$ for air-water system and also the liquid flooding velocities were found to decrease at higher viscosities. However the results due to Pushkina and Serokin [17], showed, contrary to Wallis results [14], the critical air velocity was independent of hydraulic diameter D and the flooding correlation was given for tube

diameter greater than 9 mm as K ≃ 0.3 where K is Kutateladze number

$$K = V_g \left[\frac{\rho_g^2}{g\sigma(\rho_f-\rho_g)}\right]^{1/4} . \qquad (2.2)$$

However, their data for the tubes with a diameter of less than 9 mm gave K values lower than 3.2. Similarly the studies [49] made on different tube size showed that the flooding velocity were independent of tube diameters greater than 5.08 cm (2 in). Lovell [18] showed that in large size tubes, diameter 6 inches and above, the critical Kutateladze number for zero penetration depth was between 3.13 and 3.28. For small tube size, the liquid contact angle may be a factor affecting the flooding as shown by Wallis and Makkencherry [19]. Results of Shires and Pickering [20] and Grolmes et al. [21] have shown that there is small length effect of the tube as well as tube diameter effect on flooding. The diagonal cutting of the tube end was observed to increase the flooding velocities, as observed by Hewitt [30]. The destabilizing effect of viscosity and the stabilizing effect of surface tension have also been verified [23, 24]. Larger effects of tube diameter D and length L on flooding velocities are also reported [24, 14, 25]. Chung's [26] study has shown that the tapered tube end increases the flooding liquid velocity. The correlation given by Chung is $Kg^{1/2} + mK_f^{1/2} = C_{11} \tanh [C_{12}(D^*)^{1/2})]$ where D* is bond number. With nozzle type air inlet, the values of constant are m = 0.8, C_{11} = 2.11, C_{12} = 0.9 for 45^o tapered tube end and for straight flushed tube end: C_{12} = 0.8. With the air entry from lower plenum, the values of constants are: m = 0.65, C_{11} = 1.79 and C_{12} = 0.9 for tapered tube end, and for straight flushed tube end: C_{12} = 0.8. For smooth entry end, the tube diameter effect was insignificant. Recently, the experimental studies by Bharathan [36, 37]

have shown that the interfacial shear stress is an important parameter in flooding. For given pipe, the interfacial shear stress can be quantitatively described by an empirical "interfacial friction factor" which is a function of only the mean liquid film thickness. For small tubes ($D^* < 20$), the limiting fluxes of each phase were found to be well correlated by the Wallis correlation. For large tubes the initial gas flux approached an asymptotic value of $K_g = 4.2$.

2.2 Analytical Approaches

Basically two approaches have been attempted in theoretical modelling of flooding viz., (1) flooding takes place as a result of the formation of an unstable wave on the liquid film which grows rapidly until it bridges the tube [27, 28, 23], (2) flooding as a result of a balance between gravity and interfacial shear on the film [21, 22, 31, 33]. In the first category four types of instabilities which, single or in combination, can lead to flow waviness or a change in flow pattern, are the Kelvin-Helmholtz, the Rayleigh-Taylor, the Tollmien-Schlichting and the Bernard instabilities. The standing wave model given by Shearer and Davidson [27] and the linearized small-perturbation stability analysis leading to Orr-Sommerfeld equation by Centinbudaklar and Jameson [28] have been of little success, as they failed to give a single flooding correlation. The consideration of Kutateladze [29] has shown that for interface stability, the ratio between the dynamic head and the surface tension is an important parameter, under small viscosity situation. The ratio is given as $K = \rho V^2 \delta/\sigma$, where ρV^2 is the dynamic head in contact with other phase, δ is the characteristic dimension of the flow structure given by $\delta = (\sigma/g(\rho_f - \rho_g))^{1/2}$. Thus the ratio K,

called Kutateladze number. Pushkin and Serokin [31] showed in their experimental results that the critical K value around 3.2. The flooding criteria obtained by using potential flow theory derived by Imura et al. [14], is

$$V_g + V_f = \sqrt{\frac{\sigma}{\rho_g}\left[K - \frac{1}{R-\delta}\right]} \tag{2.3}$$

where δ is film thickness. Chung [26] arrived at flooding correlation, neglecting the curvature effect of the tube again using potential flow model as:

$$K_g^{1/2} + K_f^{1/2} = C \tag{2.4}$$

where the application of kinematic wave theory was used. The results correlated by both of these authors with respective experimental data agreed quite well.

In the second category of approach, with hanging film model, Grolmes et al. [21] used Navier-Stoke equation in deriving flooding correlation. An analysis by Wallis and Kuo [34] on hanging film using potential flow equations gave the critical K_g around 1.87. The critical K_g, obtained in general was predicted to depend on contact angle of liquid into tube wall. Ueda and Suzuki [35] model considered interaction between the large amplitude wave on the liquid falling down a vertical rod and the upward gas stream at the onset of flooding. The correlation obtained theoretically, compared well with experimental data for flow inside a tube. Bharathan [36] has given a simple theoretical model for infinitely long tube with negligible end effects. Here the equations of the force balance on the gas core and on entire tube cross-section yield a relation that determines an upper limit to

countercurrent flows given as:

$$\frac{2f_i j_g^{*2}}{\alpha^{5/2}} + \frac{2f_w j_f^{*2}}{(1-\alpha)^2} = (1-\alpha) \qquad (2.5)$$

The interfacial and wall friction factors f_i and f_w can be determined from experimental data. Recently Teital et al. [33] using the similar force balance equations along with kinematic wave analysis, deduced flooding points, that agreed with results of Bharathan [37] and Hewitt et al. [38].

2.3 Flooding with Condensation

English et al. [39] performed steam-water flooding tests in a single tube updraft partial condenser made of jacket 1.83 m length and D=1.91 cm stainless steel tubes with four different diagonal tube end cutting ($\theta = 0^\circ$, 30°, 60°, and 75°) (see Table 3 for correlation). The θ angle of diagonal cutting, was found to have a stabilizing effect on the flooding velocities. An equation often used in industry [39] is the Andale equation:

$$j_g = 9.0\ (0.8)\ D^{0.67}/\rho_g^{0.5} \qquad (2.6)$$

with diagonal end cut the factor 0.8 is dropped. A proposed correlation by Diehl and Koppany [40] for steam-water system is

where for $F_1F_2(\sigma/\rho_g)^{0.5} > 10$, $A = B = 1.0$

and for $F_1F_2(\sigma/\rho_g)^{0.5} \leq 10$, $A = 0.71$, $B = 1.15$

Also: $F_1 = D/(\sigma/80)^{0.4}$ for $D/(\sigma/80) < 1.0$

and $F_1 = 1.0$ for $D/(\sigma/80) \geq 1.0$

$F_2 = (\rho_f/j_f/\rho_g j_g)^{-0.25}$

The subcooling effect of liquid on flooding in PWR down comer geometrics showed [41] an increase in the liquid flooding velocities. The correlation given by Block and Crowley [41] which takes in to account the subcooling effect is

$$j_g^{*1/2} + m j_f^{*1/2} = C \qquad (2.7)$$

where $j_f^* = \rho_f \, j_f^{1/2} \, [(\rho_f - \rho_g) g W]^{-1/2}$, W is the average annulus circumference and

$$j_g^* = j_{gc}^* + j_{gw}^* - j_{gcond}^*$$

$$j_{gcond}^* = f(T_{sat} - T_f) \frac{C_p}{h_{fg}} \left(\frac{\rho_f}{\delta_g}\right)^{1/2} j_{f,in}^*$$

and $f = \left[\frac{P}{Pa}\right]^{1/4} \left[\frac{1}{1 + b j_{f,in}^*}\right]$ is the fractional condensation efficiency. The factor b has a value 30 for cylindrical vessel and Pa is the atmospheric pressure, j_{gc}^* is steam flux generated from the core, j_{gw}^* is generated from the down comer wall and $j_{f,in}^*$ is the rate of liquid injection into the wall. With C = 0.32 in eqn. (2.7), m = exp [-5.6 $j_{f,in}^{*0.6}$]. Tien [42] has discussed a flooding correlation of this kind and he has pointed out the hysteresis behaviour with subcooling on flooding. Jones [43] studies on PWR fuel bundles showed the adequacy of subcooled flooding model given by Tein [42]. Recent studies by Wallis et al. [44] showed a correlation (2.1) holds for water-steam flow system with C=0.69 to 0.8 depending on the end conditions and m ≃ 1, and for some end conditions, fluid combinations and experimental procedures m ≃ 1.82.

2.4 Other Considerations

There are various other factors that are to be considered on flooding correlations. Hewitt [30] showed that the tube inclination has a complicated effect on flooding. Dukler and Smith [22] observed the onset of liquid entrainment associated with the onset of flooding. Chung [26] showed that the liquid entrainment reduces the flooding velocities. It is also required to see the multichannel effect on flooding; however, most of the present work in this context are with simplicity of models which in practical cases may not hold. Hence it remains a need for improving the analytical modelling of the flooding phenomena and as well to investigate the effects of various parameter affecting the flooding by experiments, such as condensation effects, liquid entrainment, multichannel flooding, surface tension and viscosity effects, effects of steam - noncondensable mixture ratio, effect of external forces, the tube length, the heat removable rates, etc.

As stated in the beginning of the present chapter, the criterion for the flooding point has been taken different by each experimental investigator. Referring to the definitions of degree of flooding presented in Chapter 1, we find that the criterion of beginning of flow reversal corresponds to the transition to flooding, the partial flooding represents the liquid entrainment, and the zero liquid penetration corresponds to that of total flooding.

Another interesting point to note while comparing the flooding phenomena studied by experiments with that by analytical approaches, is that in the analytical methods the flooding correlation obtained is based on the assumption that the flooding occurance is point wise. While the experimental observations are based on integral over the

entire system. Hence from this fundamental difference in defining the flooding point makes a considerable discrepancy between the two approaches.

CHAPTER 3

FLOODING CORRELATION WITH ELECTRIC FIELD

3.1 Introduction

The survey of flooding correlation in Chapter 2 shows that the flooding phenomena in counter-current vertical two-phase flow, in presence of external field influences such as electric field or magnetic field, has not been studied so far. However, the application of electric field to enhance heat transfer in two-phase flow systems such as boiling, condensation, has already been suggested, as discussed in Chapter 1. Here, in this chapter, the analytical modelling of flooding mechanism in counter-current gas-liquid vertical flow system under an electric field acting perpendicular to the interface is studied.

From the survey on the flooding correlations in Chapter 2, it is clear that the very mechanism of the occurrence of flooding is attributed to the interface instability. The surface waves associated with the interface, in absence of the gas and liquid velocity in the system of our interest are mainly due to gravitational field (gravity wave) and surface tension (capillary wave). With gas or liquid velocity, the waves associated with the interface will be enhanced and for higher flow rates of either phase, there could result instability leading to flooding. In analytical modelling of flooding, the potential flow equations have been successfully used [23,26,29]. In stationary systems of two inviscid fluids, it has been found that the interaction is considered on the interface deformation [50]. Hence, the interactions in the bulk of fluid due to electric field is neglected.

3.2 Equations of Motion

The counter-current flow is approximated as two immiscible inviscid streams of density ρ_ℓ and ρ_g fluid flowing counter-current to each other in a long channel. An electric field is acting perpendicular to the interface. With the two fluid streams having constant velocity U_ℓ and U_g, the annular flow is approximated as shown in Fig. 3.1a with liquid film thickness δ and the tube radius R. Small disturbances in the flow are assumed which are being generated due to fluid velocities and the applied electric potential acting on interface.

Hence, the equations of motion are given as

Continuity: $$\nabla \cdot \vec{V} = 0 \tag{3.1}$$

Momentum: $$\rho[\frac{\partial \vec{V}}{\partial t} + \vec{V} \cdot \nabla\vec{V}] + \nabla p = \rho g \tag{3.2}$$

Electrical: $$\nabla \times \vec{E} = 0 \tag{3.3}$$

$$\nabla \cdot \beta \vec{E} = 0 \tag{3.4}$$

Here, the gas and liquid are assumed to be dielectric fluids with no free charges on interface.

The interface between two fluids is represented analytically by [51].

$$F(x,y,z,t) = 0 \tag{3.5}$$

With surface variation on (y,z) plane represented by function $\xi(y,z,t)$ as shown in Fig. 3.1b the interface can be described as

$$F(x,y,z,t) = x - \xi(y,z,t) = 0 \tag{3.6}$$

The normal vector $\vec{n}$ to the interface is given by the geometry of the interface alone and is

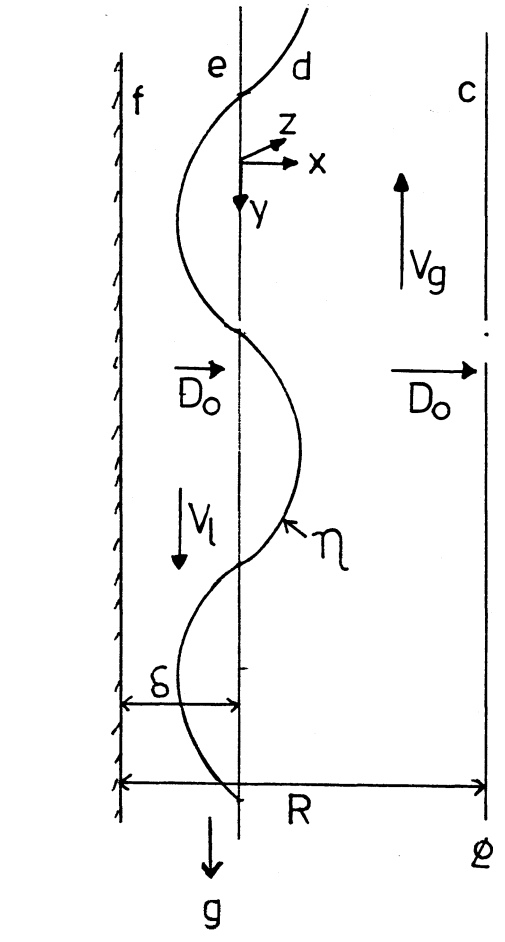

(a)

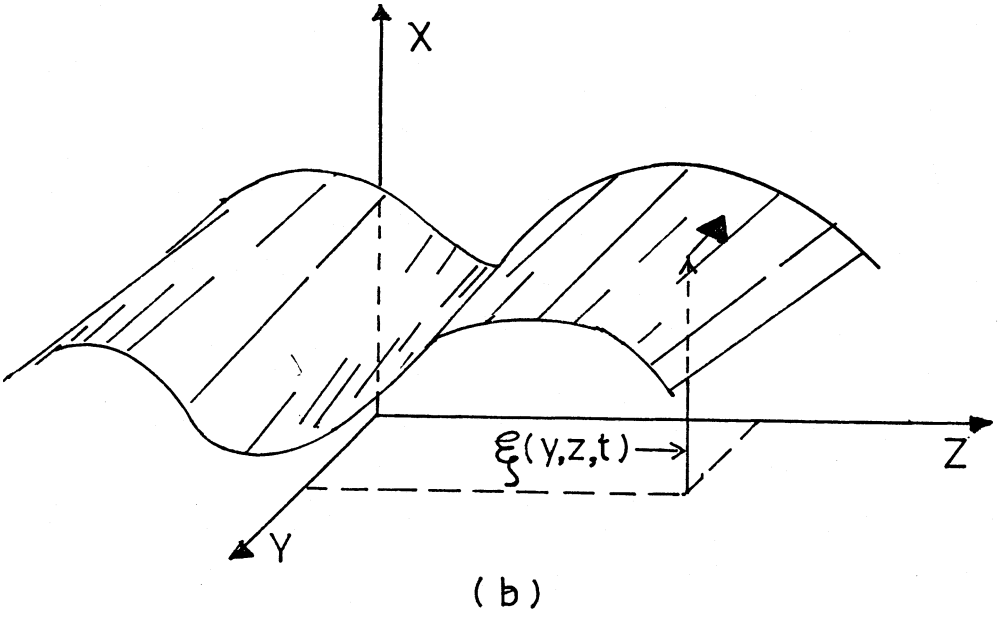

(b)

Figure 3.1 a) Geometry of the system

b) coordinates for interface

$$\vec{n} = \frac{\nabla f}{|\nabla F|} \tag{3.7}$$

Since the rate of change of F for an observer on the interface must be zero, we have

$$\frac{DF}{Dt} = \frac{\partial F}{\partial t} + \vec{V} \cdot \nabla F = 0 \tag{3.8}$$

3.3 Perturbation Analysis

Here, we employ a perturbation analysis assuming that there is an equilibrium condition of the dependent variables which satisfies the equations of motion together with appropriate boundary conditions. The amplitude of variations of variables from this equilibrium are small. Hence, the so-called "linearized perturbation" equations of motion that result from the neglect of all products of perturbation variables except the first order, are considered in the present analysis.

Each of the dependent variables appearing in Eqs. (3.1) to (3.8) is assumed to be represented by a series of the form

$$V = V_{(0)}(x,y,z,t) + V_{(1)}(x,y,z,t)\eta + V_{(2)}(x,y,z,t)\eta^2 + \ldots \tag{3.9}$$

where η is a parameter used to indicate the amplitude of the associated dependent variable. Here, η is taken to be small so that the series can be approximated by the first-order term substituting the series of the form Eq. (3.9) in the momentum equation (3.2) the x-component of equation is given by

$$\eta^0\left(\frac{\partial V_{x(0)}}{\partial t} + \vec{V}_{(0)} \cdot \nabla V_{x(0)} + \frac{\partial P_{(0)}}{\partial x} + \rho g\right)$$

$$+ \eta^1\left(\frac{\partial V_{x(1)}}{\partial t} + \vec{V}_{(0)} \cdot \nabla V_{x(1)} + \vec{V}_{(1)} \cdot \nabla V_{x(0)} + \frac{\partial P_{(1)}}{\partial x}\right)$$

$$+ \eta^2\left(\frac{\partial V_{x(2)}}{\partial t} + \vec{V}_{(0)} \cdot \nabla V_{x(2)} + \vec{V}_{(1)} \cdot \nabla V_{x(1)} + \vec{V}_{(2)} \cdot \nabla V_{x(1)} + \frac{\partial P_{(2)}}{\partial x}\right)$$

$$= 0 \tag{3.10}$$

Since each term in the parameters in Eq. (3.10) is required to vanish, we find the zero-order equations as just the equations of motion themselves. The solutions of this zero-order equations are

$$\xi_{(0)} = 0,$$

$$\vec{V}_{(0)} = 0, \tag{3.11}$$

$$P_{(0)} = -\rho g x - \frac{\rho U^2}{2} - H + c$$

$$\vec{E}_{(0)} = E_{(0)} \vec{i}_x$$

Here, c and E_0 are constant for both gas and liquid media, and H is the pressure due to external force (e.g. electric field). From Eq. (3.11), we find that the first order equations of motions are the same as the complete set of equations of motion, except that Eq. (3.2) no longer includes the convective part $(\vec{V}\cdot\nabla)\vec{V}$ and the body force $-\rho g$. Here, the first order solutions are assumed to be of the form

$$\begin{aligned} \vec{V}_{(1)} &= \mathrm{Re}[\hat{V}_x(x)\vec{i}_x + \hat{V}_y(x)\vec{i}_y + \hat{V}_z(x)\vec{i}_z] \exp\{j(\omega t - k_y y - k_z z)\} \\ P_{(1)} &= \mathrm{Re}\ \hat{P}(x) \exp\{j(\omega t - k_y y - k_z z)\} \\ E_{(1)} &= \mathrm{Re}[\hat{e}_x(x)\vec{i}_x + \hat{e}_y(x)\vec{i}_y + \hat{e}_z(x)\vec{i}_z] \exp\{j(\omega t - k_y y - k_z z)\} \end{aligned} \tag{3.12}$$

so that all other first-order variables can be written in terms ofs the first-order pressure P(x) and one component of the electric field $e_z(x)$.

Now it is apparent that we can represent the electric field in respective region (gas or liquid) as having the form of an equilibrium plus a perturbation.

$$\vec{E} = \begin{Bmatrix} E_\ell \\ E_g \end{Bmatrix} \vec{i}_x + \vec{e} \qquad \nabla e = -\nabla\phi \tag{3.13}$$

with $\vec{e} = \hat{e}_x \vec{i}_x \exp\{j(\omega t - k_y y - k_z z)\}$

and the pressure can be written in a similar way

$$P = \begin{cases} -\rho_g g x - \frac{1}{2}\rho_g U_g^2 - H_1 + c_1 + p'(x,y,zt) & x > 0 \\ -\rho_\ell g x - \frac{1}{2}\rho_\ell U_\ell^2 - H_2 + c_2 + p'(x,yzt) & x < 0 \end{cases} \tag{3.14}$$

with $p' = \hat{Re}p(x) \exp\{j(\omega t - k_y y - k_z y)\}$.

The electric field intensity is confined to the interface, where it acts on the equilibrium interface as a normal surface force density. In the bulk regions, the electric field is uncoupled from the fluid mechanics. Thus, the perturbation mechanics of each layer is described by the inviscid pressure-velocity relations [51] ($k \equiv \sqrt{k_y^2 + k_z^2}$):

$$\begin{bmatrix} \hat{p}^c \\ \hat{p}^d \end{bmatrix} = \frac{j(\omega - k_z U_g)\,\rho_y}{k} \cdot \underline{A} \cdot \begin{bmatrix} \hat{V}_x^c \\ \hat{V}_x^d \end{bmatrix}$$

$$\begin{bmatrix} \hat{p}^e \\ \hat{p}^f \end{bmatrix} = \frac{j(\omega - k_z U_g)\,\rho_\ell}{k} \cdot \underline{B} \cdot \begin{bmatrix} \hat{V}_x^e \\ \hat{V}_x^d \end{bmatrix} \tag{3.15}$$

where

$$\underline{A} = \begin{bmatrix} -\mathrm{Coth}(R-\delta)k & \frac{1}{\sinh(R-\delta)k} \\ \frac{-1}{\mathrm{Sinh}(R-\delta)k} & \mathrm{Coth}(R-\delta)k \end{bmatrix} \qquad \underline{B} = \begin{bmatrix} -\mathrm{Coth}\delta k & \frac{1}{\sinh\delta k} \\ \frac{-1}{\sinh\delta k} & \mathrm{Coth}\delta k \end{bmatrix}$$

Similarly, the perturbation electric field can be described by the field-potential transfer relations [51].

$$\begin{bmatrix} \hat{e}_x^c \\ \hat{e}_x^d \end{bmatrix} = k \cdot \underline{A} \cdot \begin{bmatrix} \hat{\phi}^c \\ \hat{\phi}^d \end{bmatrix}$$

$$\begin{bmatrix} \hat{e}_x^e \\ \hat{e}_x^f \end{bmatrix} = k \cdot \underline{A} \cdot \begin{bmatrix} \hat{\phi}^e \\ \hat{\phi}_f \end{bmatrix} \tag{3.16}$$

Now considering the boundary conditions, we have

$$\hat{V}_x^c = 0$$
$$\hat{\phi}^c = \Phi' \tag{3.17}$$

where Φ' is the electrical potential at c and at the interface, the velocities are related to the interfacial deformation

$$\hat{V}_x^e = \hat{V}_x^d = j\omega\hat{\xi} \tag{3.18}$$

The stress balance at the interface is obtained as

$$[-\rho_g g\xi + c_1 + p'(x=\xi) - \frac{1}{2}\rho_g U_g^2 - H_1(x=\xi)]$$

$$- [-\rho_\ell g\xi + c_2 + p'(x=\xi) - \frac{1}{2}\rho_\ell U_\ell^2 - H_2(x=\xi) = \sigma(\frac{\partial^2\xi}{\partial y^2} + \frac{\partial^2\xi}{\partial z^2})$$

$$- [\frac{1}{2}\beta_g(E_g + e_x^e)^2 - \frac{1}{2}\beta_\ell(E_\ell + e_x^d)^2]_{x=\xi} \tag{3.19}$$

Now for the condition of equilibrium, we should have at $x = \xi$

$$(c_1 - H_1) - (c_2 - H_2) = \frac{1}{2}(\varepsilon_g E_g^2 - \varepsilon_\ell E_\ell^2) = \frac{1}{2} D_o(E_g - E_\ell) \tag{3.20}$$

And hence, from Eq. (3.19), the perturbation part becomes the required jump condition representing stress balance at the interface

$$(\hat{p}^d - \hat{p}_e) = \hat{\xi}\, g(\rho_\ell - \rho_g) + \frac{1}{2}(\rho_\ell U_\ell^2 - \rho_g U_g^2)$$
$$= D_o(\hat{e}_x^d - \hat{e}_x^e) = k^2\sigma\hat{\xi} \tag{3.21}$$

Now, equations (3.18) and (3.21) show that the mechanical laws are satisfied at the interface. Similarly, on the electrical side, we have boundary condition at the interface

$$\vec{n} \cdot (\beta_\ell E_\ell - \beta_g \vec{E}_g)_{x=\xi} = 0 \tag{3.22}$$

and also

$$\beta_g \hat{e}_x^d = \beta_\ell \hat{e}_x^e \tag{3.23}$$

with $\vec{n}$ given by (3.7), we have from (3.22)

$$\hat{\phi}^d - \hat{\phi}^e = \hat{\xi}(E_g - E_\ell) \tag{3.24}$$

The other boundary conditions at the wall are

$$\hat{V}_x^f = 0 \tag{3.25}$$

$$\hat{\phi}^f = 0 \tag{3.26}$$

Now, by substituting the values of $\hat{p}$ and $\hat{e}_x$ in the equations (3.21), (3.24) and (3.23) from Eqs. (3.18) and (3.15) and using the boundary conditions (3.17), (3.18), (3.25) and (3.26), we have the equation (3.21), (3.24) and (3.23) respectively given as

$$\begin{bmatrix} X & kD_o\text{Cothk}(R-\delta) & kB_o\text{Cothk}\delta \\ E_g - E_\ell & -1 & +1 \\ 0 & \beta_g k\text{Cothk}(R-\delta) & \beta_\ell k\text{Cothk}\delta \end{bmatrix} \cdot \begin{bmatrix} \hat{\xi} \\ \hat{\phi}^d \\ \hat{\phi}^e \end{bmatrix} = \begin{bmatrix} \dfrac{D_o k\,\Phi'}{\sinh k(R-\delta)} \\ 0 \\ \dfrac{\beta_g\, k\,\Phi'}{\text{Sinhk}(R-\delta)} \end{bmatrix}$$

where

$$X = \frac{\omega^2}{k}[\rho_g\text{Coth}(R-\delta)k + \rho_\ell\text{Cothk}\delta] - g(\rho_\ell - \rho_g) - k^2\sigma$$

$$- 2\omega[\rho_\ell U_\ell\text{Cothk}\delta - \rho_g U_g\text{Coth}(R-\delta)k]$$

$$+ \rho_\ell U_\ell^2\text{Cothk}\delta + \rho_g U_g^2\text{Cothk}(R-\delta)$$

The solution for the amplitude of the interface is given

$$\hat{\xi} = -\frac{K\,D_o(\beta_\ell - \beta_g)\,\text{Coth}(k\delta)\cdot\Phi'}{\text{Sinh}(R-\delta)k[\beta_\ell\text{Cothk}\delta + \beta_g\text{Coth}(R-\delta)k]} \cdot \frac{1}{D(\omega,k)} \tag{3.28}$$

where

$$D(\omega,k) = X - \frac{k\,D_o(\beta_\ell - \beta_g)^2}{\beta_\ell\beta_g[\beta_\ell\,\tanh k(R-\delta) + \beta_g\,\tanh k\delta]}$$

Hence, we obtain the dispersion relationship when the instability is set on the interface due to field coupling, i.e., $\hat{\xi} \to \infty$ or $D(\omega,k)$.

Thus, we have from (3.28) the dispersion relationship given with

($c = \frac{\omega}{k}$: wave speed)

$$c^2 - cV'_{\ell g} + V''^2_{\ell g} = V_a^2 + V_c^2 - V_b^2 \qquad (3.29)$$

where

$$V'_{\ell g} = \frac{(\rho U)_{eff}}{\rho_{eff}} ,$$

$$V''^2_{\ell g} = \frac{(\rho U^2)_{eff}}{\rho_{eff}} ,$$

$$V_a^2 = \frac{\rho_\ell - \rho_g}{\rho_{eff}} \frac{g}{k} ,$$

$$V_c^2 = \frac{\sigma k}{\rho_{eff}} ,$$

$$V_b^2 = \frac{kD_o^2(\beta_\ell - \beta_g)^2}{\beta_\ell \beta_g [\beta_\ell \tanh k(R - \delta) + \beta_g \tanh k\delta]}$$

$$(\rho U)_{eff} = 2\rho_\ell U_\ell \mathrm{Coth} k\delta - 2\rho_g U_g \mathrm{Coth} k(R - \delta)$$

$$(\rho U^2)_{eff} = \rho_\ell U_\ell^2 \mathrm{Coth}\delta + \rho_g U_g^2 \mathrm{Coth}\, k(R - \delta)$$

An alternative approach of arriving at the dispersion relationship with potential flow model is presented in the Appendix, which is simpler compared to the rigorous derivation given above. Now from equation (3.29), we can find the field coupled surface wave speed c. The one way of stating the condition for instability associated with interface is that when c becomes imaginary. From equation (3.29), we find that c can become imaginary if U_ℓ and U_g are high enough or the electric field is sufficiently high. In the absence of electric field, the instability corresponds to Kevin-Helmholtz type instability. Thus, the condition for instability in the present case is given as

$$(\rho U)^2_{eff} \geq -4\ \rho_{eff}\{(\rho_\ell - \rho_g)\ \frac{g}{k} + \sigma k - \frac{f'_e}{k} - (\rho U^2)_{eff}\} \qquad (3.30)$$

Here, $f'_e = kV_b^2\ \rho_{eff}$.

From (3.30), it is evident that for a given U_ℓ and U_g, there is a certain value of electric field for which this LHS exceeds the value of RHS in eq. (3.30) and hence, the instability would result. Here, instability makes the interface wave amplitude to grow infinitely so that the flow of either phase is retarded. We reckon this point as the total flooding point in the counter-current flow system, according to the definitions of flooding described in Chapter 1. From the above equation for given liquid velocity U_ℓ and the applied electric field intensity, there is a certain value of U_g after which we have imaginary roots for wave speed. Thus with increase in gas velocity flow instability would occur and subsequently total flooding is possible. From the expression obtained for the dispersion relationship, we find that the channel width and the wavelength are determining factors in flooding. In order to explore all possible combinations of wavelength and the film thickness ratios, which are important for the onset of instability in the flow, we consider the following cases:

Case 1: ($\delta > \lambda_c$) If the average film thickness is considerably greater than the vertical wavelength λ_c (which will be considered later), then we approximate

$$\begin{aligned} &\text{Cothk}(\eta - \delta) \tilde{\sim} 1 \\ &\text{Cothk}(\eta - R + \delta) \tilde{\sim} 1 \end{aligned} \qquad (3.31)$$

So equation (3.29) reduces to

$$\rho_\ell(c - \bar{U}_\ell)^2 + \rho_g(c + \bar{U}_g)^2 - (\rho_\ell - \rho_g)\ \frac{g}{k} - \sigma k + \frac{f'_e}{k} = 0 \qquad (3.32)$$

where $f'_e/k = (\beta_g - \beta_\ell)^2 E_g E_\ell/(\beta_g + \beta_\ell)$ (no free charge).

Physically this case represents the situation where the surface wave exists over the thick film and in flooding with large liquid flow rates.

Case 2: ($\lambda_c > \delta, R$) When the wavelength is very large compared with the channel width and the average film thickness, then we have

$$\text{Cothk}(\eta + \delta) \simeq \frac{1}{k(\eta + \delta)}$$

$$\text{Cothk}(\eta - R + \delta) \simeq \frac{1}{k(\eta - R + \delta)} \tag{3.33}$$

And equation (3.29) becomes

$$\rho_\ell (c - \bar{U}_\ell)^2 \frac{1}{\eta + \delta} + \rho_g (c + U_g)^2 \frac{1}{\eta - R + \delta} - \sigma k + f'_e - (\rho_\ell - \rho_g)\frac{g}{k} = 0 \tag{3.34}$$

where

$$f'_e = \frac{(\beta_g - \beta_\ell)^2 E_g E_\ell}{\beta_g(\eta + \delta) + \beta_\ell(\eta - R + \delta)} \qquad \text{(no free charge)}$$

Case 3: ($\lambda_c \simeq \delta$) When the flow is in between the two extreme cases considered above, then we can write

$$\text{Coth } k(\eta + \delta) = c_3 \frac{R}{\eta + \delta}$$

$$\text{Coth } k(\eta - R + \delta) = c_3 \frac{R}{\eta - R + \delta} \tag{3.35}$$

where c_3 is constant.

Then, equation (3.29) becomes

$$\rho_g \frac{R}{\eta - R + \delta} (c + \bar{U}_g)^2 + \rho_\ell \frac{R}{\eta + \delta} (c - \bar{U}_\ell)^2 + \frac{1}{c_5}\left[-\frac{g(\rho_\ell - \rho_g)}{k} - k\sigma + \frac{f'_e}{k}\right] = 0 \tag{3.36}$$

where

$$\frac{f'_e}{k} = \frac{(\beta_g - \beta_\ell)^2 E_g E_\ell}{\beta_g(\eta + \delta) + \beta_\ell(\eta - R + \delta)} \qquad \text{(for no free charge)}$$

and

$$\frac{f'_e}{k} = \beta_\ell E_\ell^2/(\eta + \delta) + \beta_g E_g^2/(\eta - R + \delta) \qquad \text{(with free charge)}$$

To relate the wavespeed c to the known mean flow velocity, $\bar{U}$, the kinematic wave theory of Lighthill and Whiteman [52] is used, where we write

$$c = \bar{U} + h\left(\frac{\partial U}{\partial h}\right) \tag{3.37}$$

Here, h - is the local depth of the fluid, U - the velocity at any axial location of the channel, $\bar{U}$ - channel velocity. Hence,

$$\rho_g(c + \bar{U}_g)^2 = \rho_g\left[-\bar{U}_g - (\eta - R + \delta)\frac{\partial U_g}{\partial(\eta - R + \delta)} + \bar{U}_g\right]^2$$

$$= \rho_g \bar{U}_g^2(\eta - R + \delta)^2\left[\frac{\partial}{\partial \eta}\left(\frac{U_g}{U_g}\right)\right]^2 \tag{3.38}$$

In the present case the fluid superficial velocities are considered; hence, we can write the for the geometry of the system

$$\frac{U_g}{\bar{U}_g} = \frac{R - \delta - \eta}{R - \delta} \qquad \text{and} \qquad \frac{U_\ell}{\bar{U}_\ell} = \frac{\eta + \delta}{\delta} .$$

then,

$$\rho_g(c + \bar{U}_g)^2 = \rho_g \bar{U}_g^2(R - \delta - \eta)^2\left(\frac{1}{R - \delta}\right)^2$$

$$= \rho_g \bar{U}_g^2\left[\left(1 - \frac{2\eta}{R - \delta} + \frac{\eta^2}{(R - \delta)^2}\right)\right] \tag{3.39}$$

Similarly, for liquid phase, we obtain,

$$\rho_\ell (c - U_\ell)^2 = \rho_\ell \bar{U}_\ell [1 + \frac{2\eta}{\delta} + \frac{\eta^2}{\delta^2}] \tag{3.40}$$

Now, by putting (3.329) and (3.40) in equation (3.36), we have after some simplification,

$$\rho_g \frac{j_g^2}{\varepsilon_g^3} (1 - \frac{2\delta^*}{\varepsilon_g}) + \frac{\rho_\ell j_\ell^2}{(1 - \varepsilon_g)^3} (1 + \frac{2\delta^*}{1 - \varepsilon_g})$$

$$= \frac{1}{c_3}\{\frac{g(\rho_\ell - \rho_g)}{k} + k\sigma - \frac{f'_e}{k}\} \tag{3.41}$$

where we have used $\delta^* = \eta/R$, $j_\ell = (1 - \varepsilon_g)\bar{U}_\ell$, $j_g = \varepsilon_g U_g$ and $\varepsilon_g = (R-\delta-\eta)/R \rightarrow$ void fraction.

3.4 Flooding Correlation

By applying the maximization principle which states that the flooding phenomenon is an extreme case of counter-current flow motion and it represents the upper limit of the steady state operation. Thus, for eq. (3.41) to be valid for any δ^*, we should have

$$\frac{\rho_g j_g^2}{\varepsilon_g^4} = \frac{\rho_\ell j_\ell^2}{(1 - \varepsilon_g)^4} \tag{3.42}$$

Hence, (3.41) reduces to

$$\frac{\rho_g j_g^2}{\varepsilon_g^3} = \frac{\rho_\ell j_\ell^2}{(1 - \varepsilon_g)^3} = \frac{1}{c_3} [\frac{g(\rho_\ell - \rho_g)}{k} + k\sigma - \frac{f'_e}{k}] \tag{3.43}$$

Elimination of ε_g in (3.43) results in an equation given by

$$[\rho_g^{1/2} j_g]^{1/2} + [\rho_\ell^{1/2} j_\ell]^{1/2} = [\frac{1}{c_3} (\frac{g(\rho_\ell - \rho_g)}{k} + k\sigma - \frac{f'_e}{k})] \tag{3.44}$$

For case 1, we have a similar equation given by

$$[\rho_g^{1/2}\, j_g]^{2/3} + [\rho_\ell^{1/2}\, j_\ell]^{2/3} = \left[\frac{g(\rho_\ell - \rho_g)}{k} + k\sigma - \frac{f'_e}{k}\right]^{1/3} \tag{3.45}$$

and in case 2, we have

$$[\rho_g^{1/2}\, j_g]^{1/2} + [\rho_\ell^{1/2}\, j_\ell]^{1/2} = [R\, g(\rho_\ell - \rho_g) + Rk^2\sigma - Rf'_e]^{1/4} \tag{3.46}$$

The expression of f'_e has been given for each case above earlier.

For case 1 in equation (3.45), the instability criteria in the limit gives a critical wavelength g'_c or wave number k'_c for which the RHS of equation (3.45) is minimum at $k = k'_c$, i.e.

$$k'_c = \sqrt{\frac{g(\rho_\ell - \rho_g)}{\sigma}} = \frac{1}{2\sigma}\left[\frac{\rho_\ell \rho_g (U_g + U_\ell)^2}{\rho_\ell + \rho_g} + f'_e\right] \tag{3.47}$$

Hence, equation (3.45) reduces to

$$[\rho_g^{1/2} j_g]^{2/3} + [\rho_\ell^{1/2} j_\ell]^{2/3} = \left[2\sqrt{g(\rho_\ell - \rho_g)\sigma} - \frac{f'_e\sqrt{\sigma}}{\sqrt{g(\rho_\ell - \rho g)}}\right]^{1/3}$$

or

$$K_g^{*2/3} + K_\ell^{*2/3} = \left[1 - \frac{f'_e}{2g(\rho_\ell - \rho_g)}\right]^{1/2} = c'_k \tag{3.48}$$

where $K_i^* = \rho_i^{1/2}\, j_i [4g(\rho_\ell - \rho_g)\sigma]^{1/4}$, $i = g, \ell$.

In case 2, we have the critical wave number k''_c, for the RHS of equation (3.46) to be minimum is given by

$$k''_c = \sqrt{\frac{(\rho_\ell - \rho_g)g - f'_e}{\sigma}} \tag{3.49}$$

Hence, equation (3.46) reduces to

$$[\rho_g^{1/2} j_g]^{1/2} + [\rho_\ell^{1/2} j_\ell]^{1/2} = [2R(g(\rho_\ell - \rho_g) - f'_e]^{1/4}$$

or

$$j_g^{*1/2} + j_\ell^{*1/2} = C_k'' \tag{3.50}$$

where

$$j_i^* = \left[\frac{\rho_i j_i^2}{Dg(\rho_\ell - \rho_g)}\right]^{1/2} \qquad i = \ell, g$$

and

$$C_k'' = \left[1 - \frac{f_e'}{g(\rho_\ell - \rho_g)}\right]^{1/4}$$

D = 2R = the diameter of the tube.

Now considering the equations (3.48) and (3.50), which are the flooding correlations derived respectively for case 1, when the average film thickness is considerably larger than the critical wavelength ($\lambda_c' = 2\pi/k_c'$) and for case 2, when the wavelength ($\lambda_c'' = 2\pi/k_c''$) is very large compared with the channel width and the average film thickness. In the first case, we find from relation (3.48) that the flooding correlation is independent of the channel dimension such as tube diameter. The correlation is similar to Kutateladze-type correlation, involving the surface tension term. The effect of electric field shows an enhancement of flooding phenomena. The stabilizing effects of gravity and surface tension are reflected in RHS of equation (3.48) with electric field term. In the second case, represented by equation (3.50), we find that the flooding relation depends on the tube diameter, corresponding to Wallis-type correlation. The destabilizing effect due to electric field is also observed in this case.

In Figure 3.2, we have plotted the flooding curves for different values of non-dimensional electric field for film thickness $\delta >>$ critical wavelength λ_c (case 1). The shifting of the flooding curve

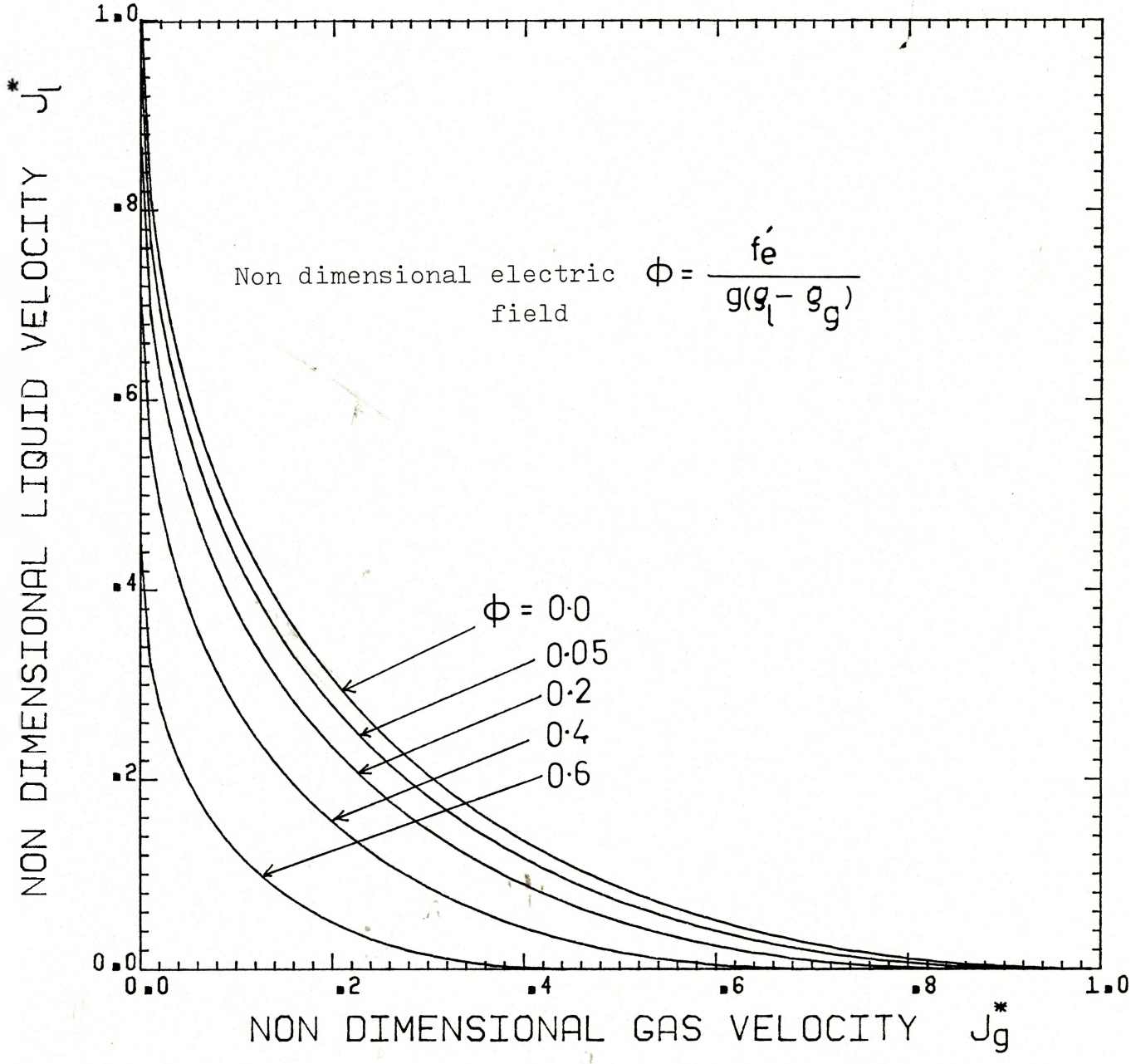

Figure 3.2 Flooding curves for case1 ($\lambda_c << \delta$) for different electric field

toward smaller j_g^* and j_ℓ^* with increasing electric field on the interface shows that the gas and liquid velocities or the flow rates decrease in presence of electric field acting on the interface in the counter-current gas liquid and flow system. In Figure 3.3, the flooding curve for critical wavelength λ_c >> film thickness and channel distance conditions (case 2) shows similar behaviour in the presence of electric field. These two cases are the representative extreme cases possible as far as the length of the critical wavelength is concerned.

At constant film thickness in the tube, the disturbance waves which grow up during unstable conditions, leading to flooding, appear such that the distance between these disturbance waves is relatively invariant with flow conditions [53]. This implies that the film thickness for particular flow conditions determines the corresponding critical wavelength. The cases 1 and 2 considered above are thus the two extreme cases possible of real situation. Hence, the practical situation would be the one that exists between the two cases. In other words, the flooding correlations would involve the dependence on the tube diameter and as well as the surface tension term.

From equation (3.44), the critical wave number in this case is given by

$$k_c'' = c_4 \nu \frac{g(\rho_\ell - \rho_g) - f_e'}{\sigma}^{1/2} \qquad (3.51)$$

where C_4 is a constant to be determined experimentally.

Now the equation (3.44) with (3.51) reduces to

$$K_\ell^{1/2} + K_g^{1/2} = C_k'' \qquad (3.52)$$

where

$$K_i = \rho_i^{1/2} \, j_i / [g(\rho_\ell - \rho_g)\sigma]^{1/4}; \qquad i = \ell, g$$

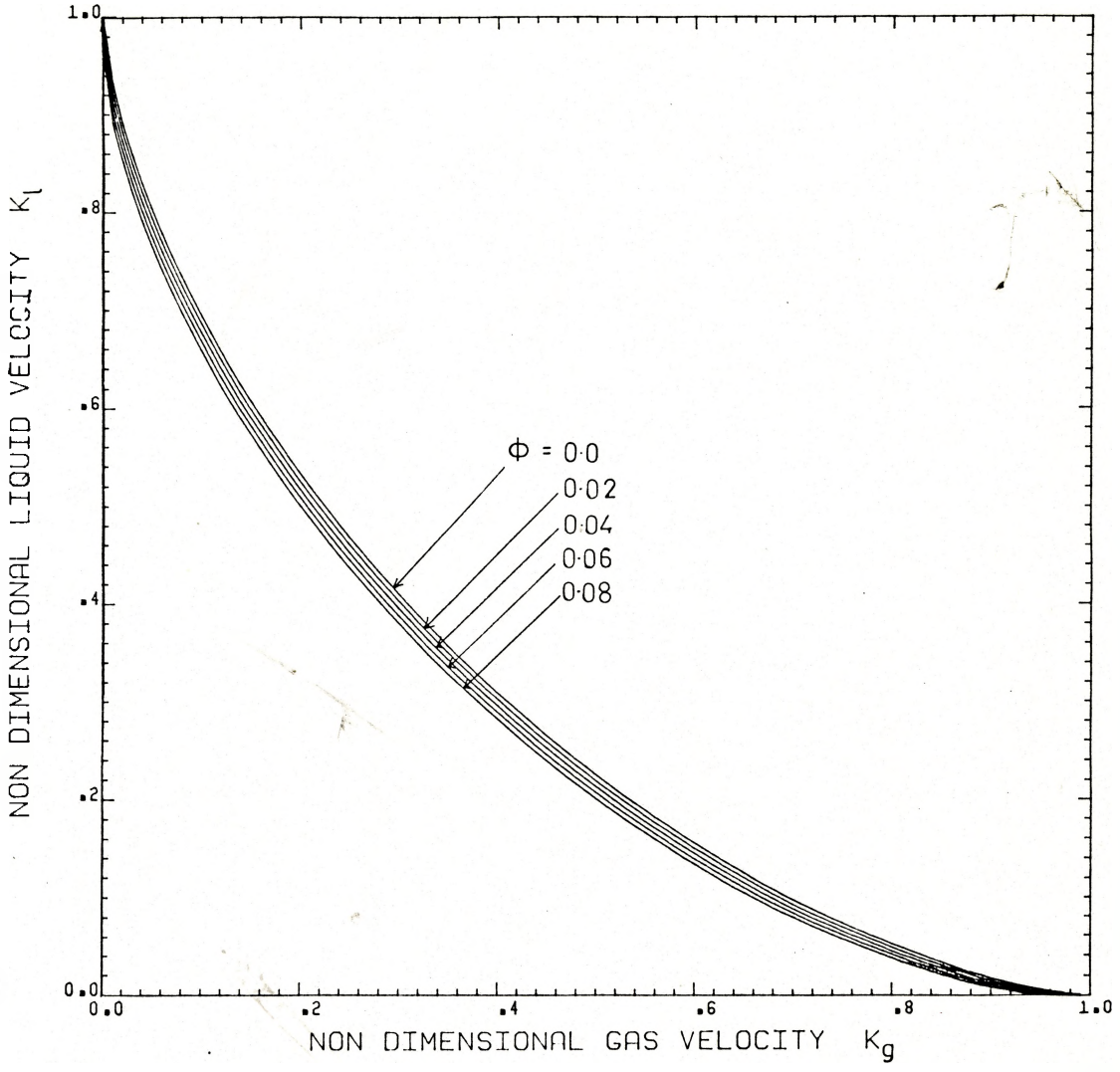

Figure 3.3(a) Flooding curves for case 2 ($\lambda_c \gg \delta$)
for small applied electric field

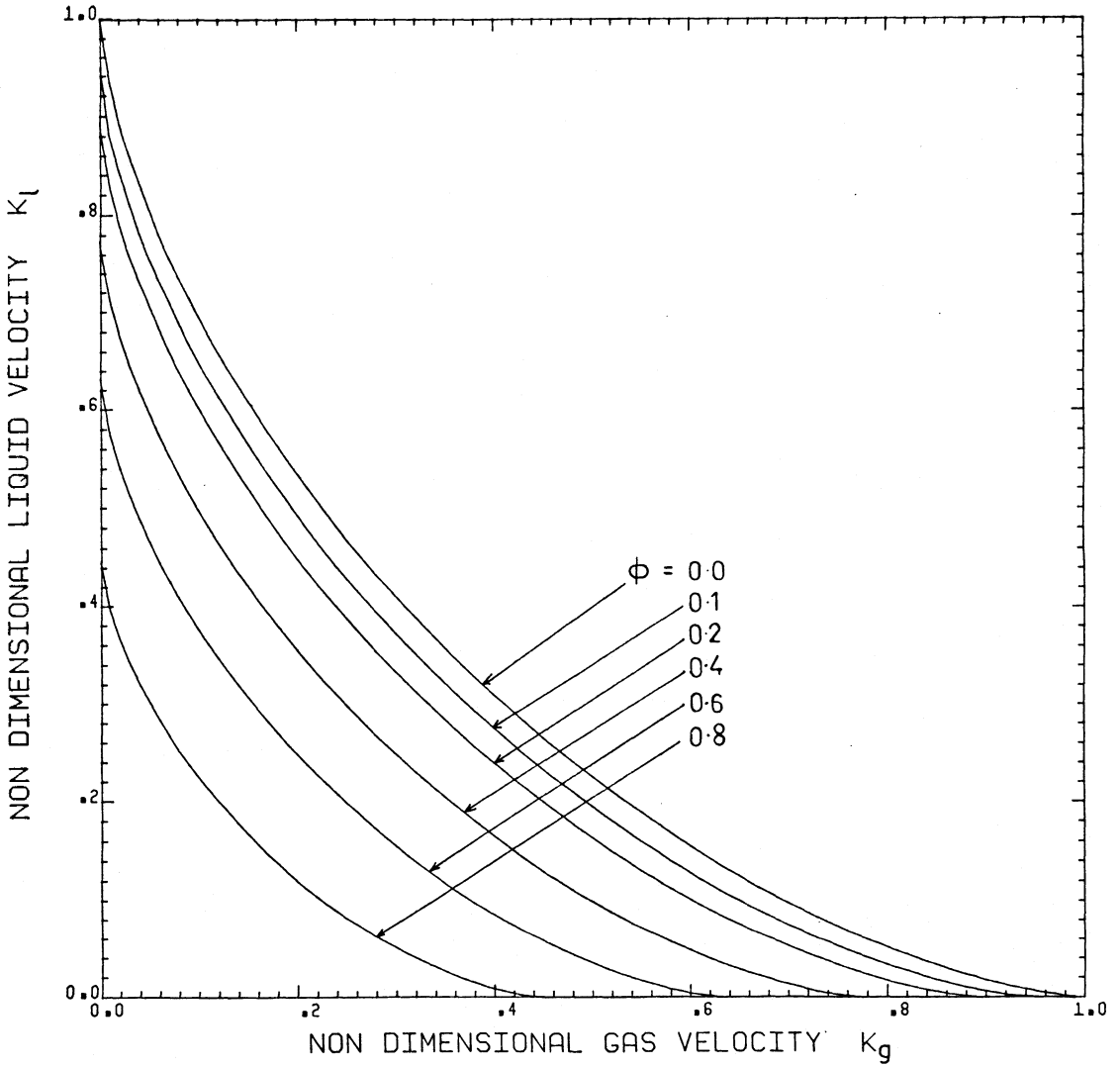

Figure 3.3(b) Flooding curves for case 2 ($\lambda_c >> \delta$)
for high values of electric field

and

$$C_k''' = \frac{1}{C_3} \{[1 - \frac{f'_e}{g(\rho_\ell - \rho_g)}]^{1/2} [C_4 + \frac{1}{C_4}]\}^{1/4}$$

Equation (3.52) shows that geometric parameters such as diameter or tube length do not appear explicitly. However, since superficial velocity j_i is a function of cross-section area, diameter or channel width plays an important role in determining the flooding limit. The length of the test channel or tube is important only when the total length of the test channel is shorter than the length between the tube inlet and the transition point. One of the consequences of the increase of the tube length is to increase the liquid film thickness at the incipient flooding point, which eventually limits the flow rate of the gas phase. Experimental studies [16,24] have indicated that the increase of tube length slightly enhances flooding. For practical applications, the pipe length is usually longer than the transition length. Therefore, flooding correlation (3.52) can be used without modifications as far as the tube or channel length is concerned. The electric field term is associated with constants C_4 and C_3, with overall effect of enhancing flooding in the system. The actual value of constant C_k''' for particular field strength depends on the configuration of the field lines on the interface as well as the tube diameter. In a system of two liquids of different conductivity having horizontal interface and with presence of a electric field acting normal to the interface, the instability has been found [50] to consist of a disturbance on the interface which, although initially sinusoidal in nature, quickly grows into a sharply pointed spout that extends toward the lighter liquid. Thus, in general, the electric field causes the

interface to be more unstable. We have seen from equations (3.48), (3.50) and (3.52) that the flooding is a result of interface instability and flow limitation. And in the presence of electric field, the interface is more unstable, and hence the flooding would occur for smaller flow rates of each phase.

The above equations (3.48), (3.50) and (3.52) were derived based on the assumption of no inlet disturbances. In a real situation, the inlet disturbances do exist, as was seen earlier in Figure 1.2, where the disturbance waves at the gas inlet would bridge the tube for higher gas velocities. These inlet disturbances cause additional head loss. It is very difficult to account for these inlet disturbances as flooding except through some semi-empirical modification of the above correlations of flooding. The general form of correlation for flooding in vertical tubes can thus be given in terms of Kutateladze-type correlations as

$$K_g^{1/2} + mK_\ell^{1/2} = C_k'' \tag{3.53}$$

where the constant m characterizes the inlet disturbances associated with falling liquid film and the gas stream. For turbulent flow, m is taken equal to unity [55]. The value of C_k'' depends on the disturbances including that due to electric field. An alternative correlation, which is a version of equation (3.354) modified by replacing the characteristic length $[\sigma/g(\rho_\ell - \rho_g)]^{1/2}$ by the tube diameter D is a Wallis-type correlation given as

$$(j_g^*)^{1/2} + m(j_\ell^*)^{1/2} = C_k'' \tag{3.54}$$

Utilizing a correlation similar to (3.53) (in the absence of electric field term), Sun [54] found that the parameter C_k'' was a constant for flooding at the upper tie plates of the boiling water reactor (BWR) fuel

bundles, he found that c was a linear function of the Bond number, a dimensionless diameter which is defined as

$$D^* = D \left[\frac{g(\rho_\ell - \rho_g)}{\sigma}\right]^{1/2} \tag{3.55}$$

Here, it can also be noted that the correlations, equations (3.48) and (3.50) obtained for cases 1 and 2 which in absence of electric field correspond to the Kutateladze form and Wallis form respectively, show that the Wallis correlation is valid for the small Bond number and the Kutateladze correlation holds for the larger Bond number case. Here, we take the convenient form of C_k''' similar to one considered by Tien et al [56] given as

$$C_k''' = (1 - \phi)^{1/8} C_5 \tanh C_6 (D^*)^{1/4} \tag{3.56}$$

Here, C_5 and C_6 are constants. Hence, the equation (3.53) reduces to

$$K_g^{1/2} + mK_\ell^{1/2} = (1 - \phi)^{1/8} C_5 \tanh C_6 (D^*)^{1/4} \tag{3.57}$$

For large D*, if we neglect the inlet disturbance so that m = 1, and in absence of electric field equation (3.57) reduces to Kutateladze equation, and hence, the constant C_5 is given as [31] $C_5 = \sqrt{3.2}$. In the other case, when $C_{12}(D^*)^{1/4}$ is sufficiently small, equation (3.57) becomes, again in absence of electric field, and m = 1, as

$$K_g^{1/2} + K_\ell^{1/2} = \sqrt{3.2}\, C_6 (D^*)^{1/4} \tag{3.58}$$

which reduces to Wallis correlation given as

$$(j_g^*)^{1/2} + (j_\ell^*)^{1/2} = \sqrt{3.2}\, C_6 = C_\omega \tag{3.59}$$

The value of C_ω is found to depend on the type of tube ends at the entrance and the way in which the liquid and gas are added and extracted. With sharp-edged flanges, $C_\omega = 0.725$, and with end effects minimized, C_ω lies between 0.88 and 1 [55].

Now, with $C_\omega = 0.725$, $C_6 = 0.4053$ and for $C_\omega = 1$, $C_6 = 0.559$. In

equation (3.57), assuming most unfavourable entry conditions, i.e. C_ω = 0.725, the flooding relation with applied electric field is

$$K_g^{1/2} + K_\ell^{1/2} = (1 - \phi)^{1/8} \sqrt{3.2} \tanh[0.405(D^*)^{1/4}] \tag{3.60}$$

Similarly, the Wallis type correlation is

$$(j_g^*)_{1/2} + (j_\ell^*)^{1/2} = (1 - \phi)^{1/8} \cdot \sqrt{3.2} \cdot C_6 = C_\omega \tag{3.61}$$

These two equations (3.60) and (3.61) are compared in Figure 3.4 for different values of non-dimensional electric field parameter ϕ. The effect of tube size on the flooding correlation shows that the higher the tube size, higher flow rates of each phase is possible. And the electric field decreases the fluid flow rate.

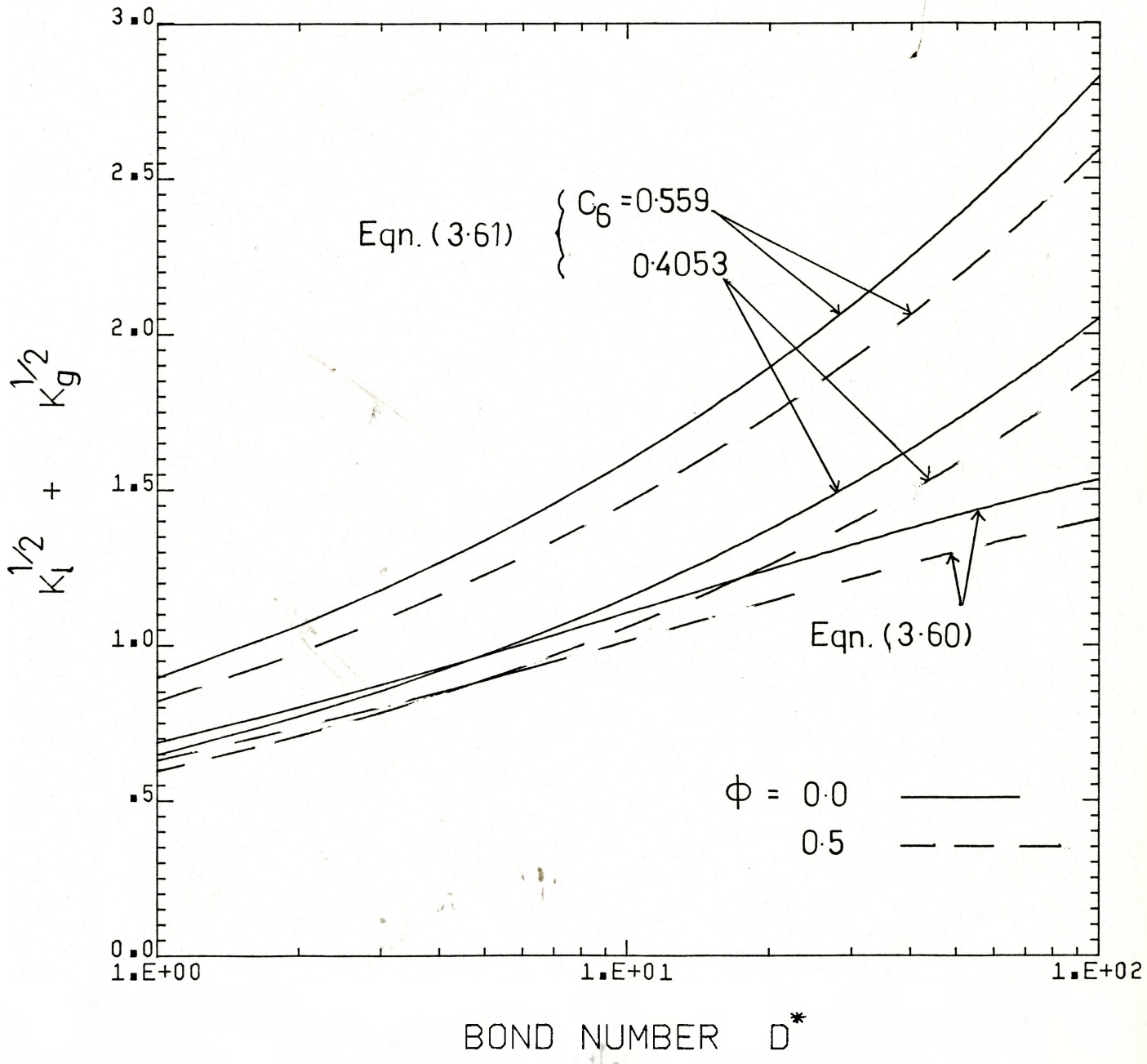

Figure 3.4 Comparison of eqs.(3.61) and (3.60) and the dependence of tube diameter.

CHAPTER 4

CONDENSATION EFFECTS ON FLOODING UNDER ELECTRIC FIELD

In the previous chapter the flooding phenomena was considered under adiabatic situation. In most of the practical cases flooding involves heat transfer as well. Such case is in the case of PWR down comer, where the condensation of saturated or superheated vapour on to a counter-current flowing subcooled liquid may reduce the effective upward steam flux. This change in upward flux of the vapour due to condensation and the condensation stress on the subcooled down flowing liquid may change the characteristics of flooding itself. Here in the present chapters the condensation effects on the counter current two-phase flooding in the presence of electric field is considered.

4.1 Subcooled Flooding Model

Flooding in the presence of heat transfer has been studied by Liu et al. [57], Segev and Collier [58] and Liu and Collier [59] for the purpose of investigating the details involved in PWR down comer thermal-hydraulics. To incorporate the effect of vapour condensation by the subcooled liquid, one of the simplest approaches is to calculate the decrease in the steam flow on the basis that the condensation latent heat is balanced by the sensible heat required to raise the temperature of the subcooled water to the saturated temperature [60]. Tien [61] has presented a simple model using this approach wherein the local change of vapour volumetric flux is given as

$$K_{ge} = K_g - B.f.\ \Delta T_{sub} \qquad (4.1)$$

where B is the property constant defined by $B = (C_p/h_{fg})(\rho_f/\rho_g)^{1/2}$ and f

is an empirical constant characterizing the fraction condensed, here f varies from 0.2 to 0.8 depending upon the degree of penetration [60]. Tien [61] has alluded to the possibility of hysteresis effect in the flooding curves when the steam flow was increased from zero value to the point of complete liquid by-pass and when it was decreased to zero again, for different values of the liquid subcooling. This hysteresis effect has also been observed experimentally by Liu and Collier [59].

From the flooding correlation derived in the earlier chapter involving the effect of external electric field, we have the Kutalateladze form of correlation

$$Kg^{1/2} + K_{\ell}^{1/2} = \frac{1}{C_3} \{[1 - \frac{f'_e}{g(\rho_{\ell} - \rho_g)}]^{1/2} [C_4 + \frac{1}{C_4}]\}^{1/4} \qquad (4.2)$$

Now in the presence of condensation by the subcooled liquid the correlation (4.2) can be written by substituting equation (4.1) for the effective vapour flux. K_{ge} as

$$[K_g - Bf\ \Delta T_{sub}\ K_{\ell}]^{1/2} + K_{\ell}^{1/2} = \frac{1}{C_3} \{[1 - \frac{f'_e}{g(\rho_{\ell} - \rho_g)}]^{1/2} [C_4 + \frac{1}{C_4}]\}^{1/4} \qquad (4.3)$$

Now replacing the RHS of Eq. (4.3) with an equation similar to the one considered by Tien et al. [53] we have

$$[K_g - Bf\ \Delta T_{sub}\ K_{\ell}]^{1/2} + K_{\ell}^{1/2} = (1-\phi)^{1/8}\ C_5 \tanh C_6\ (D^*)^{1/4} \qquad (4.4)$$

From earlier considerations we have the constant $C_5 = \sqrt{3.2}$ and for the case of must unfavourable entry condition $C_4 = 0.405$. Using these values of the constant as representative of some situation we have plotted in Fig. 4.1 the flooding correlation at different levels of liquid subcooling ($Bf\ \Delta T_{sub}$) and the strength of the electric field (ϕ) for Bond number $D^* = 10$. From the figure it can be observed that with higher subcooling, i.e. higher condensation rates, the effect of the

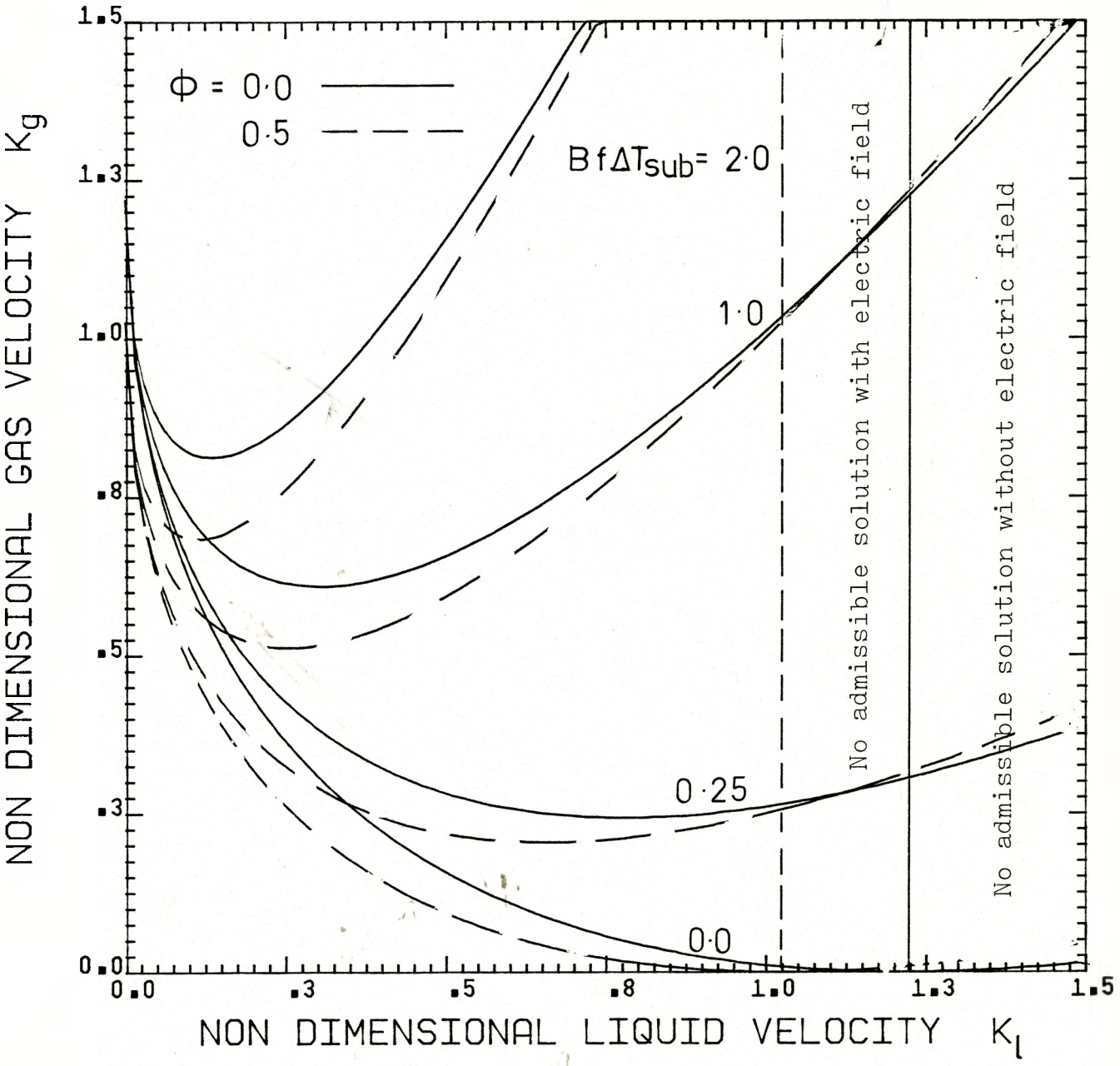

Figure 4.1 Flooding curves in presence of condensation for different subcooling and $D^*=10$

electric field appears to be high from lowest value of K_ℓ to the point of minimum of the curve. With increasing K_ℓ the effect is reducing and for the ranges of values of K_ℓ allowing admissible solutions, the total effect of the electric field is to reduce the flow rates of each phase. In Figure 4.2 we have shown the simultaneous effects of condensation and the electric field on the flooding correlation for the Bond number $D^* = 50$. Here we find the hystersis effect as has been observed by Tein [61] in the process of increasing the vapour flow rate from zero to the point of complete liquid bypass and when it was decreased to zero again. To see the effect of the Bond number on the flooding curves explicitly, in Figure 4.3, the flooding curves are plotted for non-dimensional electric field parameters $\phi = 0.5$. With increasing Bond number a larger steepening of flooding curves at low K_ℓ rates is observed.

4.2 Effect of Electric Field on Condensation

It is well known from experimental studies that the condensation heat transfer coefficient can be increased significantly by the presence of electric fields [3, 4, 62]. It has been found that this increase in heat transfer coefficient is related to the appearance of electrohydrodynamic waves on the liquid-vapour interface [4]. In the last section it has been observed that the flooding correlation under electric field with condensation of the vapour on to the subcooled liquid film, takes account of the condensation by the reduction of the steam flux rate. However in the presence of the electric field the condensation rates are higher than without electric field, it appears that the enhancement in condensation due to electric field has to be accounted in the flooding correlation.

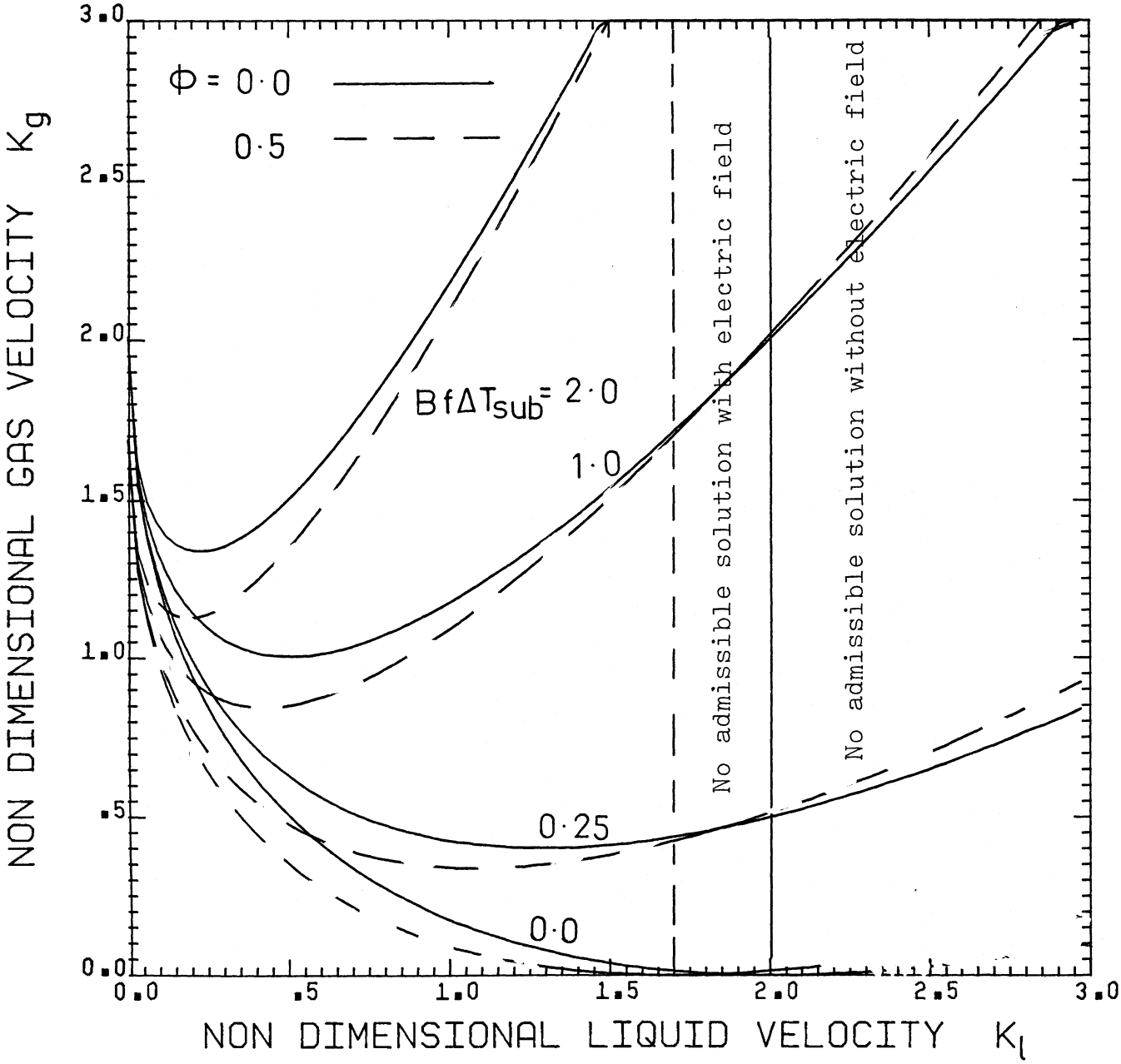

Figure 4.2 Flooding curves in presence of condensation for $D^* = 50$.

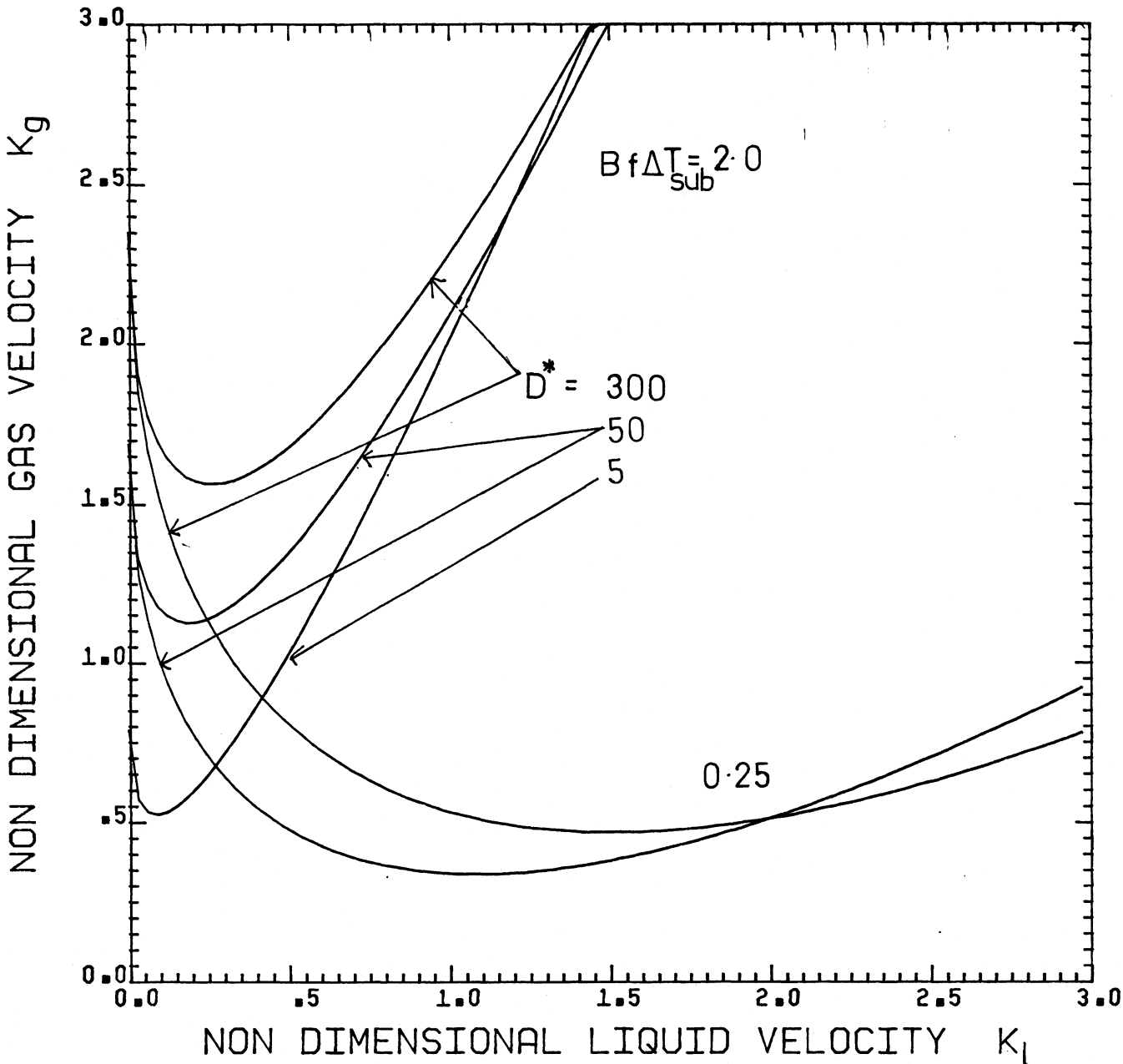

Figure 4.3 Effect of Bond number D^* on flooding curve in presence of electric field (o=0.5)

To incorporate the enhancement of condensation under electric field, in the flooding correlation, the amount of condensation increased due to the applied field has to be calculated and this has to be added to the condensed vapour and thus find the total effective reduction in vapour flux rate. For tube geometries and in case of dielectric fluid like freon the increase in heat transfer coefficients have been obtained from 2 to 10 folds with electric fields of the order of 20-60 KV [63]. But in the case of a steam-water system such a high rate of increase is not possible. Here to incorporate the effect of condensation under electric field we multiply the subcooled condensation by a parameter $z(\phi)$, which is function of the applied electric field and the system configuration as well as the fluid properties. Hence, the effective vapour flux rate is given as

$$K_{ge} = K_g - z(\phi) \cdot Bf\ \Delta T_{sub}\ K_\ell \tag{4.5}$$

Hence the flooding correlation is given as

$$[K_g - z(\phi) \cdot B \cdot f\ \Delta T_{sub}\ T_\ell]^{1/2} + K_\ell^{1/2} = (1-\phi)^{1/8}\ C_5 \tanh C_6 (D^*)^{1/4} \tag{4.6}$$

Here, z is greater than unity in the presence of electric field and when $\phi = 0$, i.e. no electric field $z = 1$. The maximum value z can take will depend upon the various factors such as the fluid properties, dielectricity, tube geometry, strength of the electric field, etc. In the case of freon experimentally, the rate of enhancement of the condensation in the presence of electric field are available in terms of heat transfer rates, i.e.

$$(h_E/h_o) = C\ (E_v/E_{cr})^m \tag{4.7}$$

where h_E, h_o are the heat transfer coefficients with and without electric field E_v is the electric field applied and E_{cr} the critical

electric field intensity after which enhancement in heat transfer is observed. For the case of Freon-113 E_c = 26 KV/cm. The value of m = 1.75. Using this information, the parameter $z(\phi)$ can be empirically given as

$$z(\phi) = \eta \, [\phi/\phi_{crit}]^{1.75} \tag{4.8}$$

where η is the factor determining the efficiency of condensation similar to the accomodation coefficient in direct contact condensation process. Assuming η unity, we find the effect of the electric field on the condensation by using the relation (4.8) in the flooding correlation (4.6). In Figure 4.4, we have shown the flooding curve for D^* = 10 and for ϕ_{crit} = 0.4. It is clear from the figure that the effect of the electric field on the condensation is to reduce the flooding point. For smaller liquid flow rates, i.e. for small K_ℓ, the enhancement of flooding due to electric field predominates. At higher liquid flow rates with subcooling (or condensation), a higher condensation due to EHD action promotes reduction of the flooding point. In Figure 4.5, we have shown the flooding curves for different degree of electric field effect on condensation, for D^* = 50 and subcooling parameter Bf ΔT_{sub} = 0.25. Thus the overall effect of the electric field is to enhance the flooding at lower liquid flow rates and dehance the flooding at the higher liquid flow rates in case of the systems involving heat transfer. This feature will be very important in practical applications where heat has to be removed by reflux condensing process such as wetted columns in chemical engineering.

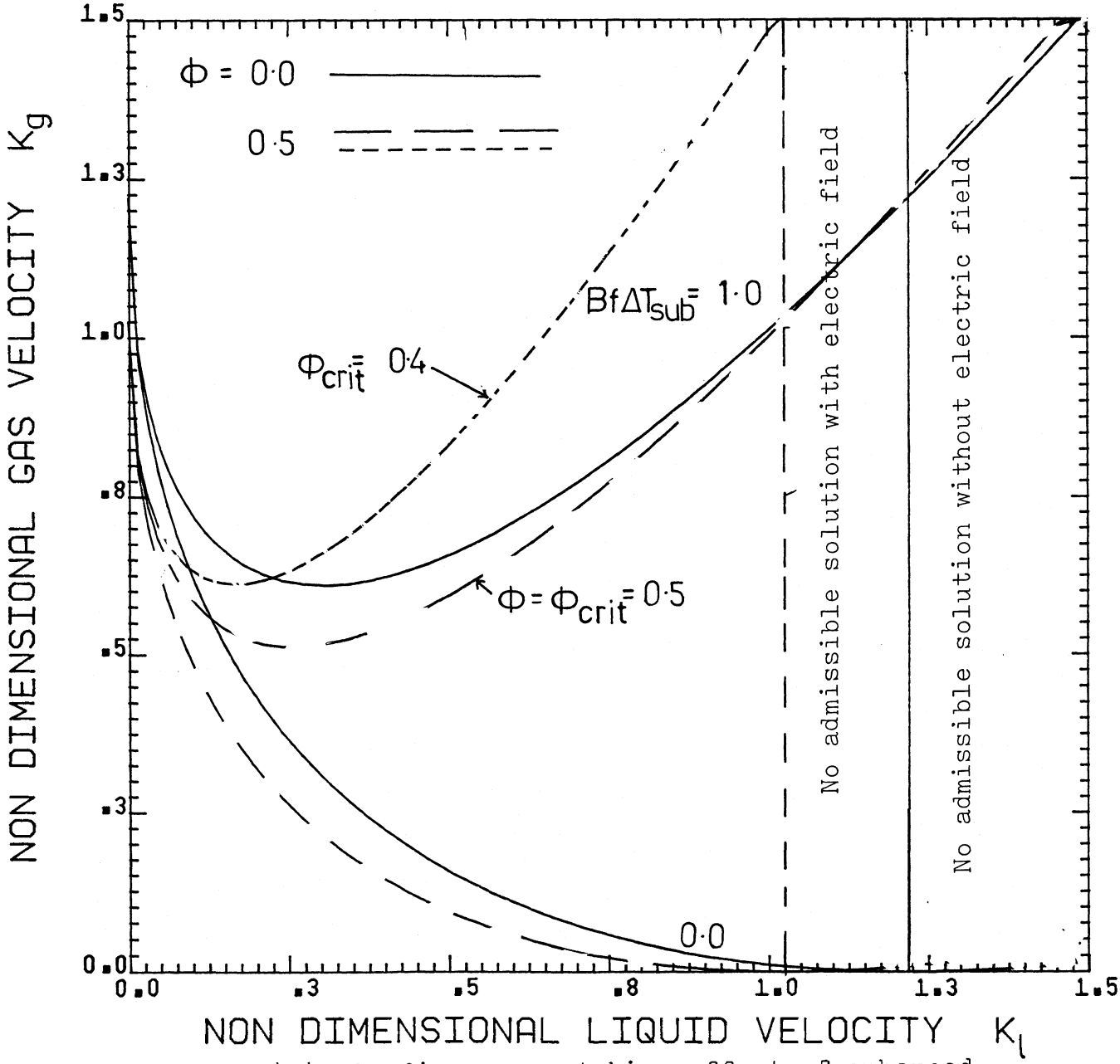

Figure .4.4 Flooding curve taking effect of enhanced condensation under electric field for D^*=10,

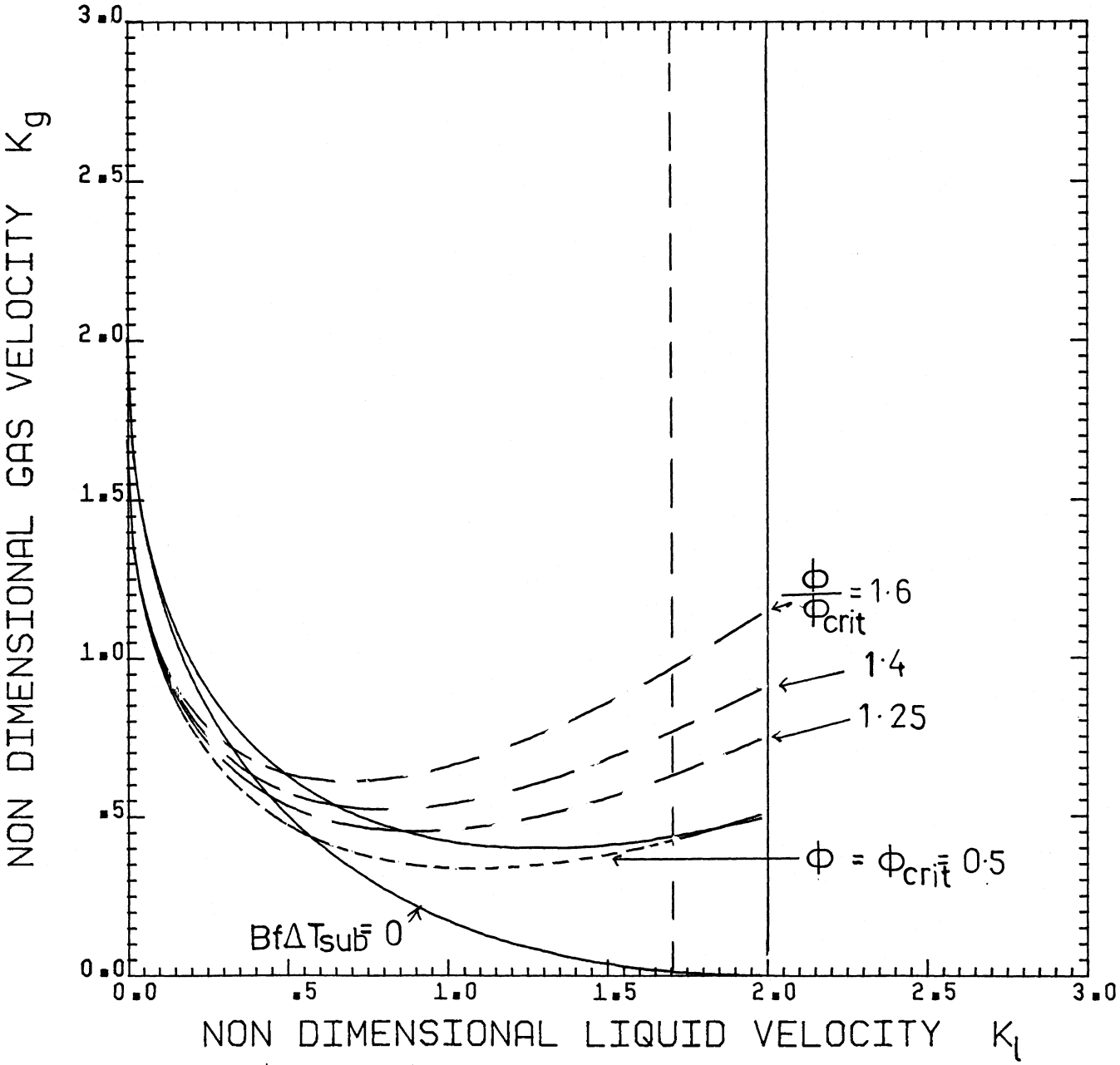

Figure 4.5 Flooding curves taking the effect of enhanced condensation for $Bf\Delta T_{sub}=0.25$ and $D^*=50$.

CHAPTER 5

DISCUSSION

5.1 Flooding Regions

From the definition of the flooding presented in Chapter 1, we find that interfacial shear stress is the restoring force in the counter-current flow dynamics, and the nature of this restoring force is dissipative type. Depending on the gas flow velocity, the shear stress will define a state for the film to be smooth or rough. The discontinuity in film thickness may occur similar to the hydraulic jump in open channel flow or normal shock in compressible gas dynamics.

For smooth film (Ref. Fig. 1.2) ($\tau_w >> \tau_i$), the wall shear stress dominates the flow of liquid. Viscous effects in the film can be characterized by an effective liquid Reynolds number.

$$Re_\Gamma = j_\ell^* N_\ell \tag{5.1}$$

where N_ℓ is the modified Reynolds number defined as

$$N_\ell = \frac{\sqrt{\rho_\ell(\rho_\ell-\rho_g)gD}\ D}{\mu_f} \tag{5.2}$$

For $Re_\Gamma < 1000$, the flow being laminar, the film thickness relation to the liquid flow is given as [8]

$$\frac{\delta}{D} = \left(\frac{3j_\ell^*}{4N_\ell}\right)^{1/3} \tag{5.3}$$

For $Re_\Gamma > 1000$, the flow is turbulent and the relation for film thickness is

$$\frac{\delta}{D} = 0.063\ j_f^{*2/3} \tag{5.4}$$

In the case with rough film ($\tau_i << \tau_w$) (Ref. Fig. 1.2), the viscous effects dominate. The viscous effects in this case are characterized by the empirical interfacial friction factor f_i given as

$$f_i = 0.005 + Fn(\delta, D, \sigma) \qquad (5.5)$$

where Fn is the function dependent on test geometry. The tube end effects are more important in this region. For the case intermediate of the above two (Region C in Fig. 1.2), the discontinuity in the flow oscillates within the tube. The amplitudes and frequencies of the flow oscillations may depend on the characteristics of air feed lines.

5.2 Applicability of Flooding Correlations

From the review presented in the second chapter, we find that a variety of correlations are available for the flooding phenomena. The major disagreement between theoretical and experimental approaches is the very definition or the criteria taken for flooding itself as indicated earlier. The flooding defined in the case of theoretical approaches isolates the system of interest and the occurence of the flooding is taken point wise. However, in the case of experimental investigations, flooding is defined on integral basis and it is the total system response that is being observed. In spite of these two fundamental differences between both approaches, even if one checks on experimental studies, the majority of the disagreements centre on the dependence of the flooding velocities on test channel geometries and on physical properties of the fluids. However the flooding correlations have been used with appropriate parametric modification suitable for a particular system. The most widely used semi-empirical flooding correlations in current LWR evaluation models are those of Wallis and of

Kutateladze-type correlations. The fundamental differences between these two correlations is the presence of the characteristic-length parameter in the Wallis correlation and the presence of surface tension in the Kutateladze correlation. These differences lead to a different scaling basis for the countercurrent flooding phenomena.

By observation of the various correlations, it is apparent that the onset of flooding in vertical tubes is more sensitive to the details of the geometry than to whether the flow is adiabatic or condensing. In deciding which correlation to use for a particular condenser design, it is advisable to compare the designed inlet geometry with those in Fig. 1. Then calculate the flooding velocity for the correlation most appropriate to that geometry irrespective of whether the correlation is for condensation or adiabatic flow. Comparison of the velocity obtained with that obtained from a correlation for condensation will enable the lower value of the two to be used for design purposes. For the cases such as tube bundle, to allow for vapour velocity variations, the designed flooding velocity can be reasonably assumed to be between 50% and 70% of the above value [48]. Experimental studies in parallel channels have indicated that Wallis correlation is of less success in applying for flooding [64, 65]. Hence, it is necessary that single-channel correlations should be modified to incorporate the multichannel effect.

5.3 Electric Field Effects on Flooding

From the correlations obtained for flooding equations (3.50) and (3.51) we observe that the magnitude of electric field parameter ϕ limits the flow rate of each phase. As seen earlier, this is mainly due

to the interaction on the gas and liquid interface, which under electric field is acted by extra force to give rise to wave shape. Even in the absence of electric field with high gas flow rates the waves appear on the interface. These waves will be enhanced in the presence of the electric field. Thus the electrohydrodynamic (EHD) growth of waves may lead to the flooding point. With large electric fields, the EHD action may produce a spraying of the liquid in the form of droplets [62]. This may add to the entrainment effects. Since in flooding, entrainment of the liquid droplets is important for very high fields, this has to be accounted in the flooding correlations.

The geometry of the flooding tube and the electric field configuration on the interface have apparently a definite effect on the disturbance created on the interface. These effects and usual tube end effects appear on the constant c terms on the RHS of equations (3.50) and (3.51). In fact, the actual values of these constants has to be determined experimentally.

In the case of condensation of the vapour, again the entrainments effects due to EHD action on the condensate film may be important. The vapour in the core region which is being transformed from dry vapour to moist vapour due to entrainment, may have its electrophysical characteristics changed. From the experimental studies it has been seen that there is variation in the pressure drop with different flux rate of the vapour in counter flow situation. The magnitude of the pressure which is uniquely related to the saturation temperature by the phase equilibrium curve, determines the electrical strength of the liquid and vapour in the system. Increase of the pressure creates the conditions for realizations of higher field intensities, promoting maximum

disturbance on the interface. These effects will be locally important.

The correlation for flooding obtained shows some constants which have to be evaluated on the basis of experimental data. The counter-current flow system of air-water with electric field applied perpendicular to the interface represent the system of present interest. To eliminate the end effects a relatively long tube with smooth inlet entry conditions is necessary. The flooding point can be defined by proper indication of pressure drop and visual tests. It will be also important to study the electrical field configuration before applying to the test system, because the concentration of field at particular point would promote higher disturbance at that point. As the EHD force is dependent on the dielectricity of the fluid used various dielectric fluid and air combinations can be tested for adiabatic cases. In the case with condensation careful experiments will be needed as the phenomena of flooding is generally associated with reflux condensation would give various flow patterns including churn flow [57].

CHAPTER 6

CONCLUSIONS

1. Four degrees of flooding have been defined in a counter-current two-phase vertical flow system by comparing the interfacial shear stress with the wall shear stress.
2. The flooding phenomenon studied experimentally and theoretically have been reviewed and the flooding correlations both for adiabatic systems and systems involving heat transfer are presented in tabular form.
3. The electric field effect on the flooding phemenoma has been studied using potential flow equations. With the application of perturbation methods, the condition for unstable interface has been derived, and a flooding correlation has been derived involving the effect of electric field acting on the interface.
4. An enhancement of flooding has been observed with applied electric field.
5. A flooding correlation has been presented for the systems involving condensation. For higher subcooling rates, the electric field effect is higher at smaller liquid flow rates.
6. The enhancement of condensation due to the applied electric field tends to bring down the flooding point, which is higher in the presence of field. Thus, the applied electric field shows two opposite effects in the same system.

REFERENCES

1. R.L. Johnson, "Effect of an Electric Field Effect on Boiling Heat Transfer", AIIA J., 6, 1457 (1968).

2. R.F. Lovenguth and D. Hanesian, "Boiling Heat Transfer in the Presence of Nonuniform, Direct Current Electric Fields", Ind. Eng. Chem. Fundam., 10, 570 (1971).

3. H.R. Velkoff and J.H. Miller, "Condensation of Vapour on a Vertical Plate with a Transverse Electrostatic Field", J. Heat Transfer, 87, 197 (1965).

4. H.Y. Choi, "Electrohydrodynamic Condensation Heat Transfer", J. Heat Transfer, 90, 98 (1968).

5. M.K. Bologa, I.A. Kozhukhar, O.I. Maradarskiy and V.D. Shkiler, "Heat Transfer in and Hydrodynamics of Electrohydrodynamic Heat Pipes", Heat Transfer-Soviet Research 12, 137 (1980).

6. R.J. Turnbull and J.R. Melcher, "Electrohydrodynamic Rayleigh-Taylor Bulk Instability", Physic. Fluids, 12, 1160 (1969).

7. K. Brunner, P.T. Wan and J.S. Chang, "Flow Regime Transitions Under Electric Fields in a Horizontal Two-Phase Flow", "Electrostatics 83", Inst. Phys. Press, London (1983) (In Press).

8. D. Bharathan, "Air-Water Countercurrent Annular Flow", EPRI Report, EPRI NP-1165, Project 443-2, Sept. 1979.

9. Banerjee, S., Chang, J-S., R. Girard and V.S. Krishnan, "Reflux Condensation and Transition to Natural Circulation in a Vertical U-Tube", ASME paper 81-WA-HT 59, pp. 1-12 (1981).

10. T.K. Sherwood, G.H. Shipley and F.A.L. Holloway, "Flooding Velocities in Packed Columns", Ind. Eng. Chem., 30, 765 (1938).

11. W.E. Lobo, L. Friend, F. Hashmall and F. Zonz, "Limiting Capacity of Dumped Tower Packings", Trans. AIChE, 41, 693 (1945).

12. S. Kamei, J. Oishi and T. Okane, "Flooding in a Wetted Wall Tower", Chem. Eng. (Japan) , 18, 364 (1954).

13. K. Feind, "Falling Liquid Films with Countercurrent Air Flow in Vertical Tubes", VDI-Forschungsheft 418, 26, 5 (1960).

14. G.B. Wallis, "Flooding Velocities for Air and Water in Vertical Tubes", UKAEA Report AEEW-R123 (1961).

15. G.B. Wallis, "The Influence of Liquid Viscosity on Flooding in a Vertical Tube", Report No. 62, GL132 (1962).

16. R. Clift, C.L. Pritchar and R.M. Nedderman, "The Effect of Viscosity on the Flooding Conditions on Wetted Wall Columns", Che. Eng. Sci., 21, 87 (1966).

17. G.B. Wallis, C.J. Crowly and J. Block, "ECC Bypass Studies", paper presented at the AIChE Symposium on LWR Safety, Boston, MA (1975).

18. T.W. Lovell, "The Effect of Scale on Two-Phase Countercurrent Flow Flooding in Vertical Tubes", M.Sc. Thesis, Dartmouth College (1977).

19. G.B. Wallis and S. Makkenchery, "The Hanging Film Phenomenon in Vertical Annular Two-Phase Flow", J. Fluids Eng., 96, 297 (1974).

20. G.L. Shires and A.R. Pickering, "The Flooding Phenomenon in Counter-current Two-Phase Flow", Symp. proceedings on Two-phase Flow, Exeter 2, B501 (1966).

21. M.A. Grolmes, G.A. Lambert and H.K. Fauske, "Flooding in Vertical Tubes", AIChE Symp. on Multiphase Flow Systems, Paper No. 38 (1974).

22. A.E. Dulker and L. Smith, "Two Phase Interactions in Counter-Current Flow Studies of the Flooding Mechanisms", NUREG-0214 (1977).

23. H. Imura, H. Kusuda and S. Funatsu, "Flooding Velocity in a Counter-Current Annular Two-Phase Flow", Che. Eng. Sci., 32, 78 (1977).

24. S. Suzuki and T. Ueda, "Behaviour of Liquid Films and Flooding in Counter-Current Two-Phase Flows - Part I, Flow in Circular Tubes", Int. J. of Multiphase Flow, 3, 517 (1977).

25. G.F. Hewitt, P.M.C. Lacet and B. Nicholls, "Transitions in Film Flow on a Vertical Tube", AERE-R4614 (1964).

26. K.S. Chung, "Flooding Phenomena in Counter-Current Two-Phase Flow Systems", Ph.D. Thesis, University of California at Berkeley (1978).

27. C.J. Shearer and J.F. Davidson, "Investigation of a Standing Wave Due to Gas Blowing Upwards Over a Liquid Film - Its Relation to Flooding in Wetted Wall Columns", J. Fluid Mech., 22, 321 (1965).

28. A.G. Centinbudaklar and G.J. Jameson, "The Mechanism of Floding in Vertical Counter-Current Two-Phase Flow", Chem. Eng. Sci., 24, 1669 (1969).

29. S.S. Kutateladze, "Elements of the Hydrodynamics of Gas-Liquid Systems", Fluid Mech. - Soviet Research, 1, 29 (1972).

30. G.F. Hewitt, "Influence of End Conditions, Tube Inclination and Physical Properties on Flooding in Gas-Liquid Flows", private communication to C.L. Tien (1977).

31. O.L. Pushkin and Y.L. Sorokin, "Breakdown of Liquid Film Motion in Vertical Tubes", Heat Transfer - Soviet Research, 4, 159 (1972).

32. G.F. Hewitt and G.B. Wallis, "Flooding and Associated Phenomena in Falling Film Flow in Vertical Tube", ASME Winter Annual Meeting, 62 (1963).

33. Y. Taitel, D. Banea and A.E. Dukler, "A Film Model for the Prediction of Flooding and Flow Reversal for Gas-Liquid Flow in Vertical Tubes", Int. J. Multiphase Flow, 8, 1 (1982).

34. G.B. Wallis and J.T. Kuo, "The Behaviour of Gas-Liquid Interfaces in Vertical Tubes", Int. J. Multiphase Flow, 2, 521 (1976).

35. T. Ueda and S. Suzuki, "Behaviour of Liquid Films and Flooding in Counter-Current Two-Phase Flow, Part 2 - Flow in Annuli and Rod Bundles", Int. J. Multiphase Flow, 4, 157 (1978).

36. D. Bharathan, "Air-Water Counter-Current Annular Flow in Vertical Tubes", EPRI Report NP-786, RP-443-2 (1978).

37. D. Bharathan, "Air-Water Counter-Current Annular Flow", EPRI Report NP-1165 RP-443-2 (1979).

38. G.F. Hewitt, P.M.C. Lacey and B. Nichols, "Transition in Film Flow in a Vertical Film", AERE-R4614.

39. K.G. English, W.T. Jones, R.C. Spillers and V. Orr, "Flooding in a Vertical Updraft Partial Condenser", Chem. Eng. Prog., 59, 51 (1963).

40. J.E. Diehl and C.R. Koppany, "Flooding Velocity Correlations for Gas-Liquid Counterflow in Vertical Tubes", Chem. Eng. Prog. Symp. Ser., 65, 77 (1969).

41. J.A. Block and C.J. Crowley, "Effect of Steam Upflow and Superheated Walls on ECC Delivery in a Simulated Multiloop PWR Geometry", Creare TN-210 (1975).

42. C.L. Tien, "A Simple Analytical Model for Countercurrent Flow Limiting Phenomena with Condensation", Letters in Heat and Mass Transfer, 4, 231 (1977).

43. D.D. Jones, "Subcooled Counter-Current Flow Limiting Characterization of the Upper Region of a BWR Fuel Bundle", NEDG-23449 (1977).

44. G.B. Wallis, D.C. deSieyes, R.J. Rosselli and J. Lacombe, "Countercurrent Annular Flow Regime for Steam and Subcooled Water in a Vertical Tube" EPRI Report NP-1336, RP-443-2 (1980).

45. N.Y. Tobilivich, I.I. Sagan and Y.G, Porzhezihskii, "The Downward Motion of a Liquid Film in Vertical Tubes in an Air-Vapour Counterflow", J. of Eng. Phys, 15, 1071 (1968).

46. V.P. Aleksiev, A.E. Poberezkin and P.V. Germsimov, "Determination of Flooding Rates in Regular Packings", Heat Transfer - Soviet Research, 4, 159 (1972).

47. C.L. Tien and C.P. Liu, "Survey on Vertical Two-Phase Counter-current Flooding", EPRI Report NP-984 RP-1160-1 (1979).

48. A.W. Deakin, "A Review of Flooding Correlations for Reflux Condensers", AERE-M-2923 (1973).

49. G.B. Wallis, C.J. Crowley and J. Block, "ECC Bypass Studies", AIChE Symp. on Light Water Reactor Safety, Boston, MA (1975).

50. J.R. Melcher, "Field Coupled Surface Waves", MIT Press, Cambridge, MA (1963).

51. J.R. Melcher, "Continuum Electromechanics", MIT Press, Cambridge, MA (1981), pp. 7.3-7.12.

52. M.J. Lighthill and G.B. Whitman, "On Kinematic Waves, I - Flood Measurement in Long Rivers", Proc. Roy. Soc. (London), 229A, 281 (1955).

53. G.F. Hewitt, "Disturbance Waves in Annular Two-Phase Flow", Proc. Inst. Mech. Engs., 184, 142 (1969-70).

54. K.H. Sun, "Flooding Correlations for BWR Bundle Upper Tie Plates and Bottom Side-Entry Orifices", 2nd Multiphase Flow and Heat Transfer Symp. Workshop, Miami Beach, FL, April 16-18 (1979), p. 1615.

55. G.B. Wallis, "One-Dimensional Two-Phase Flows", McGraw-Hill Book Company, New York (1969).

56. C.L. Tien and K.S. Chung, "Entrainment Limits in Heat Pipes", AIAA J., 17, 643 (1979).

57. J.S.K. Liu. R.P. Collier and R.A. Cudnik, "Flooding of Counter-Current Steam-Water Flow in an Annulus", in "Topics in Two-Phase Heat Transfer and Flow", S.G. Bankoff, ed., ASME, New York, pp. 107-113 (1978).

58. A. Segev and R.P. Collier, "Condensation and Vapourization Effects on Counter-Current Steam-Water Flow in an Annulus", in "Non-Equilibrium Interfacial Transport Processes", ASME, New York (1979).

59. J.S.K. Liu and R.P. Collier, "Heat Transfer in Vertical Counter-Current Steam Water Flooding Flows" in "Basic Mechanisms in Two-Phase Flow and Heat Transfer", P.H. Pothe and R.T. Lakey, eds., ASME, New York, pp. 123-129 (1980).

60. G.B. Wallis, J.S. Crowley and J.A. Block, "ECC Bypass Studies", AIChE Symp. on LWR Safety, Boston, MA (Sept. 1975).

61. C.L. Tien, "A Simple Analytical Model for Counter-Current Flow Limiting Phenomena with Vapour Condensation", Letters Heat Mass Transfer, 4, 231 (1977).

62. A.B. Didkovskii and M.K. Bologna, "Intensification of Heat Exchagne upon Condensation of a Vapour in an Electric Field", Teplofizika Vysoki Temp, 16, 576 (1978).

63. M.K. Bologa, I.A. Kozhukhar, O.I. Mardarskiy and V.D. Shkilev, "Heat Transfer in and Hydrodynamics of Electrohydrodynamic Heat Pipes", Heat Transfer - Soviet Research, 12, 137 (1980).

64. Y. Hagi, "Air-Water Flooding for Parallel Channel Flows Based on the Results for Single Path Flows", M.S. Thesis, Dartmouth College (19 76).

65. D.M. Spencer and L. Kmetyk, "Flooding in Multichannel Two-Phase Counterflow", Nuclear Reactor Safety Heat Transfer 55-62 ASME, New York (1977).

66. Y. Fuji-E, et al., IAEA Workshop on Fusion Reactor Design Problems, Culham, UK (1974).

67. J-S. Chang, "Applicaton of EHD Technique to a Nuclear Power Plant Emergency Core Cooling System", IEEE/IAS (1983), in press.

68. A.V, Chechetkin, "High-Temperature Coolants", Energiya, p. 496 (1971).

69. G.F. Hewitt, "Disturbance Waves in Annular Two-Phase Flow", Proc. Inst. Mech. Engrs., 184, P+C, 142-150 (1969-70).

APPENDIX I

The interface is assumed to be consisting of a disturbance of sinusoidal form given by (Ref. Fig. 1 in Chapter 3)

$$\eta = \eta_o \sin k(x - ct) \tag{A.1}$$

Here, η_o is the amplitude, $k = 2\pi/\lambda$, with λ - wavelength of the wave. Thus, the free surface is represented by a perturbation given by

$$y = \eta(x,t)$$

The velocity potential (ϕ_i) of each phase is expressed with small perturbation (ϕ_i') superimposed on the average values ($\bar{U}_i$), i.e.

$$\begin{aligned} \phi_g &= -\bar{U}_g x + \phi_g' \\ \phi_\ell &= \bar{U}_\ell x + \phi_\ell' \end{aligned} \tag{A.2}$$

Hence, the perturbed velocity potentials satisfy the Laplace equation as

$$\frac{\partial^2 \phi_i}{\partial x^2} + \frac{\partial^2 \phi_i}{\partial y^2} = 0 \qquad i = \ell, g \tag{A.3}$$

The pressure at each phase is expressed with Bernoulli's equation in linearized perturbed form as:

$$\frac{\rho_g'}{\rho_g} = -\frac{\partial \phi_g'}{\partial t} + \bar{U}_g \frac{\partial \phi_g'}{\partial x} = \frac{1}{2}\left\{\left(\frac{\partial \phi_g'}{\partial x}\right)^2 + \left(\frac{\partial \phi_g'}{\partial y}\right)^2\right\} + f_g'(E) \cdot \eta + c_1 \tag{A.4}$$

$$\frac{\rho_\ell'}{\rho_\ell} = -\frac{\partial \phi_\ell'}{\partial t} + \bar{U}_\ell \frac{\partial \phi_\ell'}{\partial x} = \frac{1}{2}\left\{\left(\frac{\partial \phi_\ell'}{\partial x}\right)^2 + \left(\frac{\partial \phi_\ell'}{\partial y}\right)^2\right\} + f_\ell'(E) \cdot \eta + c_2 \tag{A.5}$$

where ρ_i', f_i' are the perturbed total pressure and the pressue due to electric field respectively and c_1 and C_2 are constants. The boundary conditions are:

$$\frac{\partial \phi_i'}{\partial y} = 0 \qquad \begin{aligned} &\text{for } i = \ell, \quad y = -\delta \\ &\text{for } i = g, \quad y = R - \delta \end{aligned} \tag{A.6}$$

The conditions at the interface at $y = \eta$, are

(i) Kinematic conditions

$$\frac{\partial \eta}{\partial t} \mp \bar{U}_g \frac{\partial \eta}{\partial x} = \frac{\partial \phi_i'}{\partial y} \qquad \begin{matrix} - \text{ for } i = g \\ + \text{ for } i = \ell \end{matrix} \tag{A.7}$$

(ii) Dynamic conditions

$$p_\ell' - p_g' = -\sigma \frac{\partial^2 \eta}{\partial x^2} - f_e'(E)\eta \tag{A.8}$$

Now, we consider equations (A.4) and (A.5). The term in the parentheses { } is a quadratic term and we assume that the kinetic energy given by this term can be balanced by a disturbance originating in the component of gravity force and the electric field which acts normally to the surface of the wave.

Thus we can write

$$-\frac{1}{2}\left\{\left(\frac{\partial \phi_i'}{\partial x}\right)^2 + \left(\frac{\partial \phi_i'}{\partial y}\right)^2\right\} = -gy' - f_i'(E)y' \simeq -g\eta - f_i'(E)\eta \tag{A.9}$$

Now equations (A.4) and (A.5) reduce to

$$\frac{\rho_g'}{\rho_g} = -\frac{\partial \phi_g'}{\partial t} - \bar{U}_g \frac{\partial \phi_g'}{\partial x} - g\eta + c_1 \tag{A.10}$$

$$\frac{\rho_\ell'}{\rho_\ell} = -\frac{\partial \phi_\ell'}{\partial t} - \bar{U}_\ell \frac{\partial \phi_\ell'}{\partial x} - g\eta + c_2 \tag{A.11}$$

Assuming the perturbed velocity potential ϕ_i' can be expressed as A(x) cosk(y - ct), from equation (A.3), we find the solution of velocity potential as

$$\phi_i' = K_1 \,\text{coshk}(y + \delta)\,\text{cosk}(x - ct) \tag{A.12}$$

$$\phi_g' = K_2 \,\text{coshk}(y - R + \delta)\,\text{cosk}(x - ct) \tag{A.13}$$

where K_1 and K_2 are constants.

From the kinematic condition at the interface, equation (A.7), the constants K_1 and K_2 are obtained and hence the velocity potentials are given as:

$$\phi'_{\ell} = -\eta_o(c - \bar{U}_{\ell}) \frac{\cosh k(y + \delta)}{\sinh k(\eta + \delta)} \cos k(x - ct) \tag{A.14}$$

$$\phi'_{g} = -\eta_o(c - \bar{U}_{g}) \frac{\cosh k(y - R + \delta)}{\sinh k(\eta - R + \delta)} \cos k(x - ct) \tag{A.15}$$

Now, by substituting equations (A.14) and (A.15) into equations (A.10) and (A.11), and using dynamic condition at the interface equation (A.8), with some modifications, we find a relation as:

$$\rho_{\ell}(c - \bar{U}_{g})^2 \coth k(\eta + \delta) + \rho_{g}(c + U_{g})^2 \cosh k(\eta - R + \delta)$$

$$- (\rho_{\ell} - \rho_{g}) \frac{g}{k} - \sigma k + \frac{f'_e}{k} = 0 \tag{A.16}$$

This can be written in conventional form of dispersion relationship as

$$c_2 - cV'_{\ell g} + V''^{2}_{\ell g} = V_a^2 + V_c^2 - V_b^2 \tag{A.17}$$

where

$$V'_{\ell g} = \frac{(\rho U)_{eff}}{\rho_{eff}} ,$$

$$V''^{2}_{\ell g} = \frac{(\rho U^2)_{eff}}{\rho_{eff}} ,$$

$$V_a^2 = \frac{\rho_{\ell} - \rho_{g}}{\rho_{eff}} \frac{g}{k} ,$$

$$V_c^2 = \frac{\sigma - k}{\rho_{eff}} ,$$

$$V_b^2 = \frac{f'_e}{\rho_{eff}\, k} .$$

$$(\rho U)_{eff} = 2\rho_{\ell}\bar{U}_{\ell}\ \text{cothk}(\eta + \delta) - 2\rho_{g}\bar{U}_{g}\ \text{cothk}(\eta - R + \delta)$$

$$(\rho U^2)_{eff} = \rho_{\ell}\bar{U}_{\ell}^2\ \text{cothk}(\eta + \delta) - \rho_{g}\bar{U}_{g}^2\ \text{cothk}(\eta - R + \delta)$$

and

$$\rho_{eff} = \rho_{\ell}\ \text{cothk}(\eta + \delta) + \rho_{g}\ \text{cothk}(\eta - R + \delta)$$

TABLE 1

Flooding Correlations for Gas-Liquid System in Single Tube

Author	Fluids	Tube Diameters in cms.	Flooding Correlation
Wallis (5)	air-water	1.27, 1.91, 2.54, 5.1	$j_g^{*1/2} + j_f^{*1/2} = c$ with $j_i^* = j_i \rho_i^{1/2} [Dg(\rho_f - \rho_g)]^{-1/2}$ i=g, f & $0.725 \leq c \leq 0.875$.
Imura et al. [14]	air-water air-ethylene glycol air-n heptane	1.12, 1.60, 2.10, 2.42	$\frac{G}{L}\left(1 + \frac{G}{L}\frac{\rho_g}{\rho_f}\frac{S_g}{S}\right) = \frac{S_g}{SL}\left(\frac{\rho_g \sigma}{\delta}\right)\left(\xi - \left(\frac{1}{R/\delta - 1}\right)^{1/2}\right)^{1/2}$. where $L = \rho_f j_f S_f$, $\xi = \rho_g j_g S_g$, $S = \pi D^2/4$, $S_f = \pi D\delta(1-\delta/D)$, $S_g = (\pi D^2/4)(1-2\delta/D)^2$, $\xi = 0.046(D^2 \rho_f g/\delta)^{1/2}$, and $\delta = (3\mu_f^2/\rho_f^2 g)^{1/3} Re_f^{1/3}$ for $R_f = LD/4\,\mu_f(1-\delta/D)$ $= 0.369\,(3\mu_f^2/\delta_f^2 g)^{1/3} Re_f^{1/3}$ for $R_f > 400$.
Chung [17]	air-water	1.59, 3.18, 4.60, 6.99	$K_g^{1/2} + K_f^{1/2} = C_k$, $C_k = 2$ for 45° tapered end. Where $K = j_g \rho_g^{1/2} [g\sigma(\rho_f - \rho_g)]^{-1/4}$.
Kamei et al. [3]	air-water air-millet jelly solution air-soap solution	1.9, 3.2, 4.2, 4.9	$\frac{\rho_g j_g}{\rho_f j_f} = 198 \left(\frac{4\rho_f j_f}{\pi D \mu_f}\right)^{-1.225} \left(\frac{\sigma}{D^2 \rho_f}\right)^{-0.23} \left(\frac{\mu_g}{\mu_f}\right)^{0.71} \left(\frac{\rho_g}{\rho_f}\right)^{0.13} \left(\frac{D^3 \rho_f^2 g}{\mu_f}\right)^{0.231}$
Feind [4]	air-water	2.0, 5.0	$M\left(\frac{Re_g}{Re_f^n}\right)\left(\frac{\rho_g}{\rho_f}\right)^{2/5}\left(\frac{\mu_g}{\mu_f}\right)^{3/4)} + 1.4\times10^4 = 1300\left(\frac{R}{\delta}\right)^{5/4}$ for Ref. ≤ 400 m = 53.2, n = 1/3; for Ref. > 400 m = 157.7, n = 1/2 .
Hewitt [21]	air-water air-silicon oil air-glycerol (38% & 67%)	1.27, 3.18	$j_g^{*1/2} + j_f^{*1/2} = c$.
Pushkin & Sorokin [22]	air-water	0.62, 0.88, 0.9 1.2 and also 30.9 (with porous injection.)	$K_{Cr} = 3.2$

TABLE 1 (Continued)

Flooding Correlations for Gas-Liquid System in Single Tube

Author	Fluids	Tube Diameters in cms.	Flooding Correlation
Grolmes et al. [12]	nitrogen-water	0.4, 0.6, 1.3, 2.5	$j_g = 1.15 \left(\frac{\rho_f}{\rho_q} \frac{g\delta}{0.006 + \frac{200\,\delta^2}{(\mu/\mu_R)^{0.44}}}\right)^{1/2}$
Hewitt & Wallis [23]	air-water	3.18	$j_f^{*1/2} + j_f^{*1/2} = 1$.
Clift et al. [7]	air-water air-glycerol (25%, 59%, 70%, 77% and 82%)	3.18	$j_g^{*1/2} + 0.34 j_f^{*1/2} = 0.79$ (for air water)
Suzuki and Veda [15]	air-water air-glycerol air-sec-octynol	1.0, 1.8, 2.88	$F_r = A \log_{10} X + B$ where $X = Re_f^{-1/3} (\rho_f\, gD^2/\sigma')^{1/4} (\mu g/\mu_f)^{2/3}$ $0.76 \leq A \leq 14.86$ $\sigma' = \sigma + 15(\sigma - 0.05)$ $18.37 \leq B \leq 29.7$ $R_{ej} = \frac{\rho_f j_f D}{\mu_f}$ Higher values at $Re_f > 350$ Lower values at $Re_f \leq 350$.
Dukler and Smith [13]	air-water	5.1	$j_g^{*1/2} + j_f^{*1/2} = 0.88$
Alekseer et al. [37]			$K_{Cr} = 3.2\, Fr^{-0.22}\, We^{-0.26}$, where $Fr = Q_f(\rho_f - \rho_g)^{3/4}\, g^{-1/2}\, \sigma^{-3/4}$ $W_e = \sigma/(\rho_f - \rho_g) g\, D_{eq}^3$.
Tobilevich et al. [36]	air-water air-sugar	3.27, 5.25, 3.0.	$Fr = a \exp\{bk(\rho_g/\rho_f)^{0.2}\}$ for $Fr > 0.012$, $a = 1.29$, $b = 014.14$ for $Fr < 0.012$, $a = 0.0653$, $b = -10.12$

TABLE 2

Parametric Dependence

Gas entry condition	Smooth entry geometry and nozzle (entry) end: flooding liquid velocity increase: (17, 5, 14, 27).
Tube diameter and tube length effect	No explicit dependence for flooding velocity (12, 17, 18, 19, 20, 22) Dependence on flooding velocity: (14, 16, 5, 15, 27)
Viscosity	Destabilizing effect on flooding: (6, 21, 7, 17) Stabilizing effect on flooding: (15, 19)
Surface Tension	Stabilizing effect on flooding: (21, 17, 19) No general trend: (15)
Condensation	Stabilizing effect (32, 33, 34)

TABLE 3

Flooding Correlations Involving Condensation

Author	Fluids	Tube Diameters in cms.	Correlation
English et al. [30]	Steam-Water	1.91 cm	$\rho_g j_g = \frac{1550\, D^{0.3}\, \rho_f^{0.46} \cdot \rho_g^{0.5}\, \delta^{0.9}}{\mu_f^{0.14}\, (\cos\theta)^{0.32} \cdot \left(\frac{\rho_f j_f}{\rho_g j_g}\right)^{0.07}}$ Andale eqn: $j_g = 9(0.8)D^{0.67}/\rho_g^{0.5}$
Diehl and Koppany [31]	Steam-Water		$j_g = A\{F_1 F_2 (\sigma/\delta_g)^{0.5}\}^B$ ... (see text for details)
Block and Crowley [32]	Steam-Water		$j_g^{*1/2} + m j_f^{*1/2} = c$ (see text for details)
Tien [33]	Steam-Water		$(K_g - Bf\Delta T_{sub}\, K_f)^{1/2} + K_f^{1/2} = 1.79$ $B = \frac{C_p}{h_{fg}} \left(\frac{\rho_f}{\rho_g}\right)^{1/2}$
Jones [34]	Steam-Water		$\dot{M}_{in_c} = \frac{\dot{M}_f\, c_p \Delta T_{sub}}{h_{fg}}$ $\dot{M}_{in_c}$ - steam flow rate; $\dot{M}_f$ - liquid injection rate
Tobilevich et al. [36]	Steam-Water	3.27, 5.25, 3.0	$Fr = a \exp\{bk(\rho_g/\rho_f)^{0.2}\}$, for $Fr > 0.012$, $a = 1.29$, $b = -14.14$, for $Fr < 0.012$, $a = 0.0653$, $b = -10.12$.